IONIZATION AND RADIATIVE CORRECTIONS
TO
ELASTIC ELECTRON SCATTERING

John Alexander Gordon

United States
Naval Postgraduate School
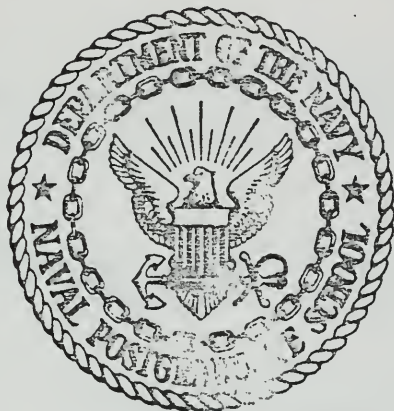
THESIS

IONIZATION AND RADIATIVE CORRECTIONS
TO
ELASTIC ELECTRON SCATTERING

by

John Alexander Gordon

June 1970

Ionization and Radiative Corrections

to

Elastic Electron Scattering

by

John Alexander Gordon
First Lieutenant, United States Air Force
B.S., University of Missouri, 1968

Submitted in partial fulfillment of the
requirements for the degree of

MASTER OF SCIENCE IN PHYSICS

from the

NAVAL POSTGRADUATE SCHOOL
June 1970

ABSTRACT

The theory of the ionization and radiative corrections to electron scattering cross sections has been reviewed to determine the formulas most valid for the experimental arrangement at the NPGLINAC. Experimentally it has been determined that the corrections most nearly account for undetected electrons when the lower limit of the measured scattering spectrum is at least four half-widths below the peak of the spectrum. It has also been found that the corrections, most likely the Bethe-Heitler correction, induce a positive error of several percent to the cross-section when thick targets are used.

TABLE OF CONTENTS

A	atomic weight
$d\sigma/d\Omega$	differential cross section
E_1	incident electron energy
E_3	energy of the elastic peak (most probable energy of the scattered electron spectrum)
E_4	$E_1 + M - E_3$
E_3'	lower limit of the electron spectrum
K_i	ionization correction
M	mass of the scattering nucleus
T	target thickness in radiation lengths ("effective" thickness)
X_o	radiation length (g/cm^2)
Z	atomic number
c	velocity of light
m, mc^2	rest energy of the electron = 0.511 MeV
$P_1 P_3$	$= 2E_1 E_3 \sin^2(\theta/2)$
P_4	$= (E_4^2 - M)^{\frac{1}{2}}$
q^2	momentum transfer
t	target thickness in g/cm^2 ("effective" thickness)
r_o	classical electron radius
Γ, Γ_b	half-width of the scattered spectrum
ΔE	$= E_3 - E_3'$

ΔE_1 resolution of the incident electron

$\Delta \Theta$ angular spread due to finite width of entrance slit

Θ scattering angle

$\bar{\Phi}(x)$ Spence function

α $= 1/137.04$

β_4 $= (E_4^2 - M^2)^{\frac{1}{2}}/E_4$

δ_B Bethe-Heitler correction

δ_S Schwinger correction

ξ Wheeler-Lamb factor

η recoil factor

η_2, η_B factors defining Γ as a function of ΔE

ρ target density (g/cm^3)

ACKNOWLEDGEMENTS

I. INTRODUCTION

Linear electron accelerators (LINAC) are well suited for the study of nuclear structure. The interaction between a nucleus and a high energy incident electron, which is entirely electromagnetic, is thought to be well understood. By momentum analyzing electrons of initial energy E_1 which are scattered through an angle θ into a solid angle $d\Omega$, one can determine the differential cross section for scattering, $d\sigma/d\Omega$. This cross section can yield much information about the charge structure of the target nuclei. Hofstadter [1,2] has written a full review of the theory and techniques of elastic electron scattering.

It is well known that these high energy electrons radiate a portion of their energy (bremsstrahlung) in the presence of nuclei or other electrons. This bremsstrahlung leads to a broadening of the scattered electron distribution such that there is a finite probability of scattered electrons with energy approaching zero. A broadening of the distribution is also due to energy loss by ionization. Since in most experiments it is not feasible to measure the spectrum down to zero energy, there is a lower energy limit to the measured spectrum. It is therefore necessary to calculate and apply corrections to the experimentally determined cross sections to account for the undetected low-energy scattered electrons.

As the precision and accuracy of scattering experiments improve, these corrections become more and more significant. If, for example, a ten percent correction were only known to ten

percent, this would result in only a one percent contribution to the uncertainty in the experimental cross section. But obviously such uncertainties are not acceptable when attempting to do an experiment to one percent accuracy.

This paper is concerned with three distinct corrections. The first of these corrects for energy loss due to Landau straggling (ionization). The other two are properly called radiative corrections. The Schwinger correction compensates for bremsstrahlung in the field of the target nucleus (scattering center) while the Bethe-Heitler correction deals with bremsstrahlung in the field of atomic electrons and other nuclei in the target. The cross section for the first process is proportional to the target thickness while for the latter it is proportional to the square of the thickness.

The following sections include a review of the theory for each of the three processes, as best suited for application at the Naval Postgraduate School LINAC (NPGLINAC), that is, for scattering experiments in the 30 to 100 MeV range where the scattered electrons are detected and momentum analyzed while the recoil nuclei are not detected. The NPGLINAC is described in detail in theses by Barnett and Cunneen [3] and Midgarden [4].

It should be noted that in actual applications the corrections are multiplicative corrections to the experimentally determined cross sections. However, to be consistent with most publications in this field, the sections concerned with the theory use the form

$$\left(\frac{d\sigma}{d\Omega}\right)_{exp} = \left(\frac{d\sigma}{d\Omega}\right) \cdot K_i \cdot S_s \cdot S_B$$

where K_i, S_s, S_B are the corrections, $\left(\dfrac{d\sigma}{d\Omega}\right)$ is the corrected cross section while $\left(\dfrac{d\sigma}{d\Omega}\right)_{exp}$ is the experimentally determined raw cross section.

Since the Bethe-Heitler correction is proportional to the square of the target thickness, its validity can be checked experimentally by measuring $\dfrac{d\sigma}{d\Omega}$ on targets of different thickness. Such experiments were performed and the results are reported. The proper applications of the corrections, for example, the choice of lower energy limit of the spectrum, have also been examined.

II. IONIZATION CORRECTION

As a monoenergetic beam of electrons passes through a scattering target the resulting spectrum of scattered electrons is broadened, in part, by ionization loss, or Landau straggling. This straggling induces an error in the cross-section determination because the scattered spectrum is not normally measured to zero energy. Thus a correction should be applied to account for these undetected electrons. This correction has largely been ignored at the NPGLINAC and other accelerators. For targets and energies encountered at the NPGLINAC, the ionization correction is typically about one percent. Until recently the accuracy of cross-section measurements was insufficient to warrant the inclusion of such small corrections. Since many cross-section measurements are made relative to another nucleus, the correction is even less important. A review of this correction is provided for completeness and possible future use.

Since in electron scattering experiments it is neither desirable nor feasible to measure the scattered spectrum down to zero energy, there is a lower energy limit of the detected spectrum, E_3', so that $\Delta E = E_3 - E_3'$. This is illustrated in Fig. 1. Thus a fraction of the spectrum, $\nu(\Delta E)$, is lost by ionization. Then the ionization correction can be expected to have the form:

$$K_i = 1 - \nu(\Delta E).$$

This is applied to the experimental cross-section:

$$\left(\frac{d\sigma}{d\Omega}\right)_{exp} K_i^{-1} = \frac{d\sigma}{d\Omega} \ .$$

Landau [5] first calculated the energy distribution of scattered electrons when monoenergetic electrons are incident on a target of thickness $t(g/cm^2)$. Following this theory, the fraction lost can be calculated by integration of the Landau function $\emptyset(\Delta E)$,

$$\nu_L(\Delta E) = 1 - \Psi(\Delta E)$$

$$\Psi(\Delta E) = \int_{E_3}^{E_o} \emptyset(\Delta E)dE \bigg/ \int_{o}^{E_o} \emptyset(\Delta E)dE.$$

A graph of $\nu_L(\Delta E)$ is given by Landau and also by Symon [6] and is reproduced as Fig. 2.

$\nu_L(\Delta E)$ has been approximated by Isabelle and Bishop [7] who have derived an expression for the correction, K_L,

$$K_L = 1 - \frac{1.21 \ a \cdot t}{\Delta E} , \qquad (2-1)$$

where $a = 0.1537 \cdot Z \cdot \rho/A \cdot \beta^2$ MeV $cm^2 g^{-1}$.

The above equation has regions of applicability which must be observed:

   a. When ΔE is of the order of $a \cdot t$ or smaller, the approximation of $\nu_L(\Delta E)$ is unsatisfactory.

   b. For very thin targets the Landau theory is only a zero-order approximation. This treatment neglects fluctuations due to distant collisions, in which the atomic electrons cannot be treated as free electrons [8].

To improve the Landau correction, Breuer [9] used $\nu_L(\Delta E)$ as given by Landau rather than the Bishop-Isabelle approximation. He also incorporated the theory of Blunk and Leisegang [10] since this
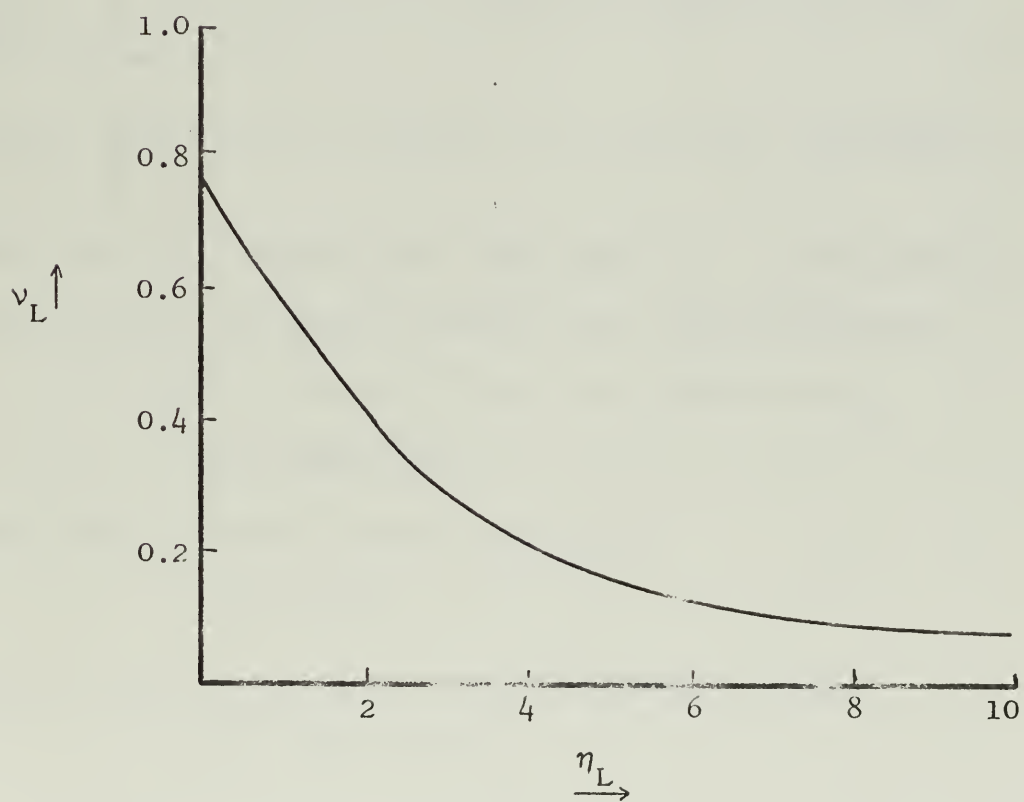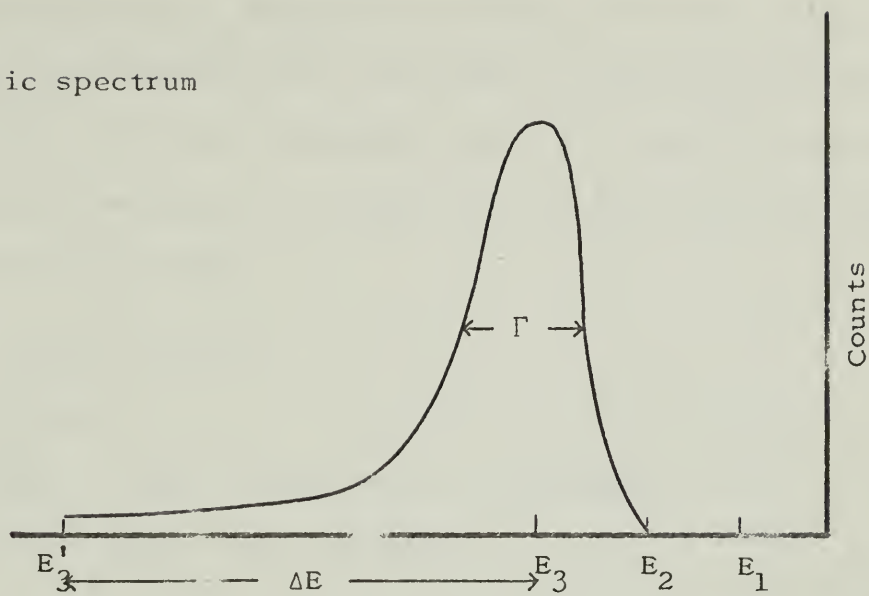
13

Fig. 1.
Typical elastic spectrum

Fig. 2. ν_L as given by Landau.

shows better agreement with experiments than the Landau theory. Since the calculations of Blunk and Leisegang introduce only a broadening of the distribution, the Landau $\nu_L(\Delta E)$ can be used by substituting the Blunk and Leisegang values for the full width at half maximum (half-width), Γ_B. Breuer has plotted this half-width as a function of b^2, where

$$b^2 = q\,\bar{Q}\,z^{4/3}/(a \cdot t)$$

$$q = 20 \text{ eV}$$

$$\bar{Q} = \bar{Q}_1 \rho t = \text{mean energy loss for thickness } t$$

$$\bar{Q}_1 = \text{mean energy loss per } g/cm^2.$$

The plot of $\Gamma_B/(a \cdot t)$ as a function of b^2 is given in Fig. 3. $\bar{Q}_1$ can be calculated by an empirical equation given by Sternheimer [11]:

$$\bar{Q}_1 = \frac{A}{\beta^2}\, t\, [B + 0.43 + \ell n\, E_1 - \beta^2 + C - a_s(X - \log_{10} p/mc)^m] \text{MeV}. \quad (2\text{-}2)$$

The empirical constants for this equation, as determined by Sternheimer, are given in Table 1 for selected targets.

The abscissa values of Fig. 3 are defined as η_L,

$$\eta_L = \Delta E/1.51 \cdot a \cdot t\ .$$

The Landau relation for the half-width,

$$\Gamma_L = 4 \cdot a \cdot t,$$

can be substituted into the above relation to give

$$\eta_L = \Delta E/(0.379\ \Gamma_L).$$

15
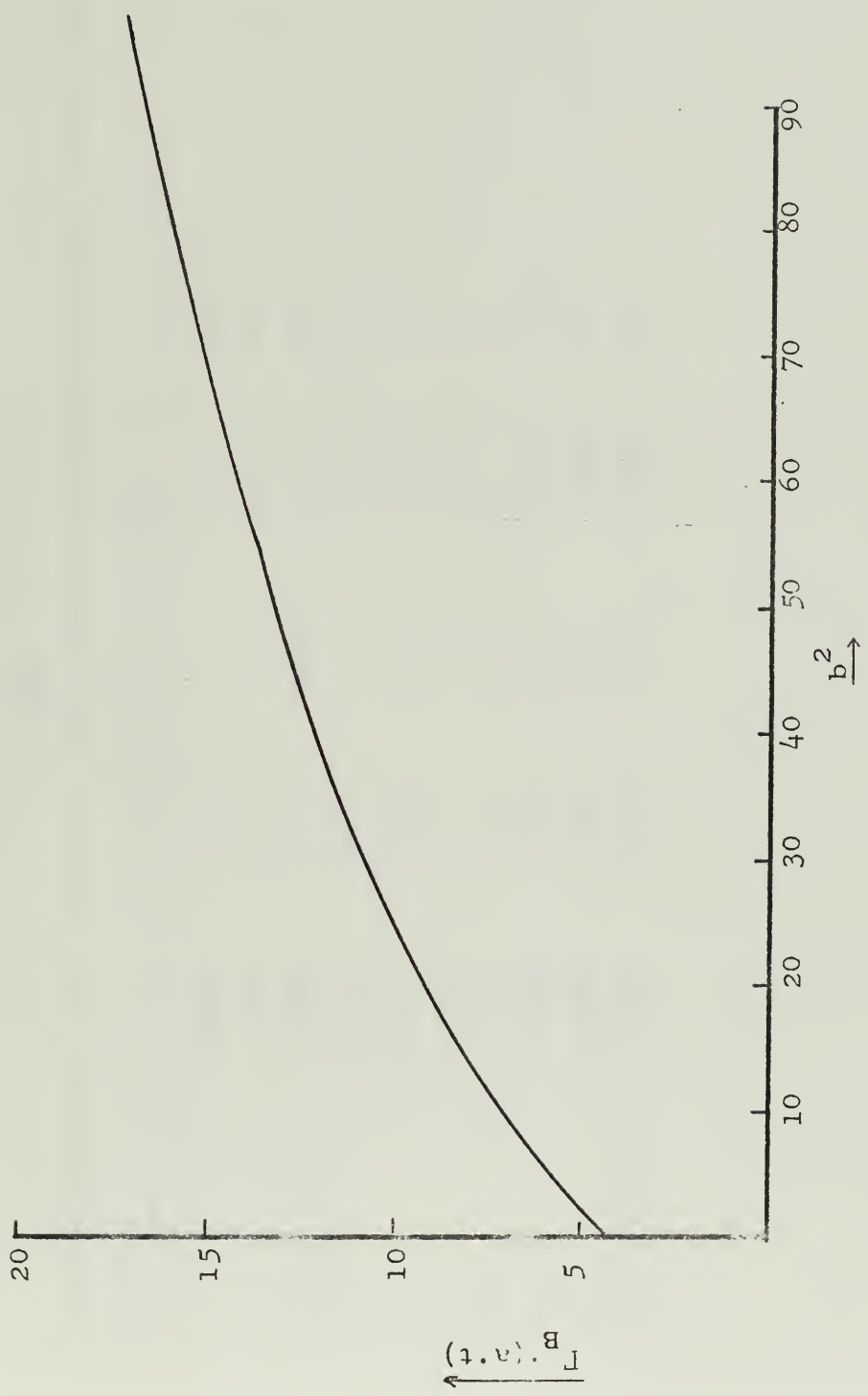
Fig. 3. Half-width Γ as predicted by Blunk and Leisegang.

16

TABLE I.

Sternheimer Empirical Constants used to calculate ionization mean energy loss

Material	A	B	-C	a_s	m	X_1
Li	0.0664	19.63	3.07	0.374	3.05	2
Be	0.0681	18.64	2.83	0.413	2.82	2
Graphite	0.0768	18.25	3.22	0.531	2.63	2
Al	0.0740	16.77	4.21	0.0906	3.151	3
Cu	0.0701	15.09	4.74	0.119	3.38	3
H_2	0.1524	21.07	9.50	0.505	4.72	3
He	0.0767	19.39	11.18	2.13	3.22	3
N_2	0.0768	17.94	10.68	0.125	3.72	4
O_2	0.0768	17.67	10.80	0.130	3.72	4
Polyethelene	0.0876	18.95	2.94	0.393	2.86	2

Now the Landau half-width should be replaced by the larger and
more correct Blunk and Leisegang half-width, Γ_B:

$$\eta_B = 2.65 \cdot \Delta E / \Gamma_B.$$

For relativistic energies and $\eta_B > 2$, $\nu(\Delta E)$ falls off inversely
with ΔE. From Fig. 2 it is seen that $\nu(\eta = 10) = 0.08$, and thus

$$1 - \nu(\eta = 10) = .92 .$$

Hence the ionization correction can finally be written as

$$K_i = 1 - \frac{0.8}{\eta_B}$$

$$= 1 - \frac{0.8}{2.65} \frac{\Gamma_B}{\Delta E} . \qquad (2\text{-}3)$$

To apply the ionization correction it is first necessary to
determine b^2 for the particular experiment. Γ_B is then determined
from Fig. 3 and substituted into the expression for K_i.

In most experiments at the NPGLINAC, $b^2 < 0.5$ so that the
Landau relation can be used:

$$\Gamma_B / (a \cdot t) \cong 4 .$$

Then

$$\eta_B = .6625 \cdot \Delta E / (a \cdot t),$$

so that

$$K_i = 1 - \frac{0.8}{.6625} \frac{(a \cdot t)}{\Delta E} . \qquad (2\text{-}4)$$

18

III. RADIATIVE CORRECTIONS

The radiative corrections to elastic scattering are of two types. The Schwinger correction, called simply the radiative correction by some authors, accounts for the emission and re-absorption of virtual photons in the field of the scattering nucleus, nuclear bremsstrahlung, as well as the emission of soft photons of energy less than a specified cutoff energy, E_3. The Bethe-Heitler correction, also called the radiation tail, accounts for the emission of real photons, by bremsstrahlung in the field of atomic electrons and in the field of nuclei other than the target nucleus.

A. SCHWINGER CORRECTION

There are several versions of the Schwinger correction, all of which are improvements on the original correction first given by Schwinger [12]. His calculations include the following assumptions:

    a. stationary nucleus

    b. Coulomb point field

    c. first Born approximation

    d. one-quantum emission

    e. $\beta = v/c \simeq 1$

with the restrictions

    a. $\Delta E << E_1 - m c^2$

    b. $E_1 \sin \frac{\theta}{2} / m c^2 >> 1$.

The Feynman diagrams corresponding to Schwinger's calculation are given in Fig. 4. This correction, δ_S, is applied as

$$\left(\frac{d\sigma}{d\Omega}\right)_{exp} = \left(\frac{d\sigma}{d\Omega}\right)\left[1 - \delta_S\right]$$

where

$$\delta_S = \frac{4\alpha}{\pi}\left[(\ln\frac{E}{\Delta E} - \frac{13}{12})(\ln\frac{2p_o}{K}\sin\frac{\theta}{2} - \frac{1}{2}) + \frac{17}{12} + \frac{1}{2}\sin^2\frac{\theta}{2}\ f(\theta)\right] .$$

This can be put into a more convenient form [13].

$$\delta_S = \frac{2\alpha}{\pi}\left\{(\ln\frac{\Delta E}{E} - \frac{13}{12})(\ln\frac{-q^2}{m^2} - 1) + \frac{17}{36} + \frac{1}{2}\ f(\theta)\right\} ,$$

where

$$f(\theta) = \ln(\sin^2\frac{\theta}{2})\ \ln(\cos^2\frac{\theta}{2}) + \Phi(\sin\frac{\theta}{2}) .$$

Φ is the Spence function[1] [14]

$$\Phi(x) = \int_o^x - \frac{\ln|1-y|}{y}\ dy .$$

To simplify calculations this is usually seen as

$$\delta_S = \frac{2\alpha}{\pi}\left\{(\ln\frac{E}{\Delta E} - \frac{13}{12})(\ln\frac{-q^2}{m^2} - 1) + \frac{17}{36}\right\} . \tag{3-1}$$

---

[1] $\Phi(x) = x + \frac{1}{4}x^2 + \frac{1}{9}x^3 + \cdots + \left(\frac{x^n}{n^2}\right) + \cdots$ if $|x| \leq 1$;

$\Phi(1) = \frac{1}{6}\pi^2$ and $\Phi(-1) = -\frac{1}{12}\pi^2$

$\Phi(x) = -\frac{1}{2}\ln^2|x| + \frac{1}{3}\pi^2 - \Phi(\frac{1}{x})$ if $x > 1$

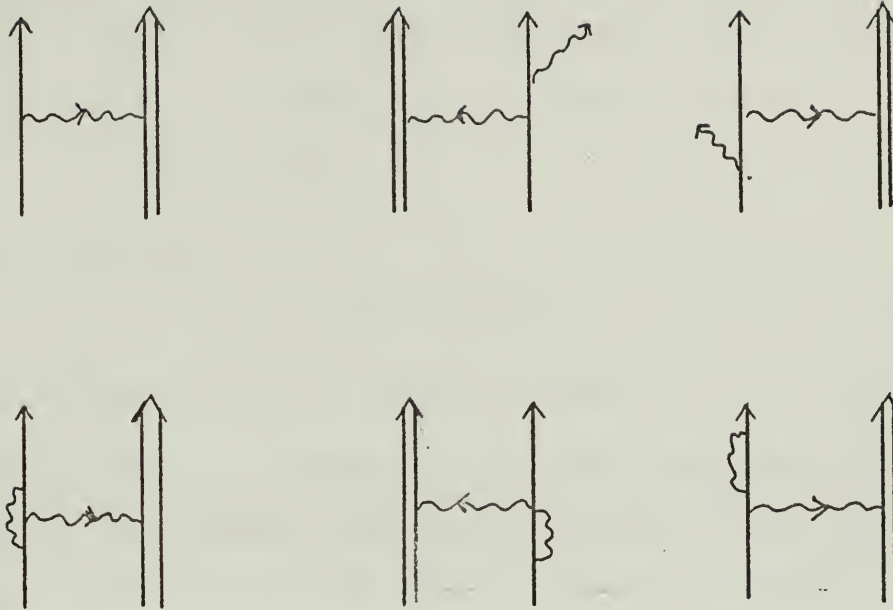$\Phi(x) = -\frac{1}{2}\ln^2|x| - \frac{1}{6}\pi^2 - \Phi(\frac{1}{x})$ if $x < -1$.

Fig. 4. Feynman diagrams corresponding to the original Schwinger correction.
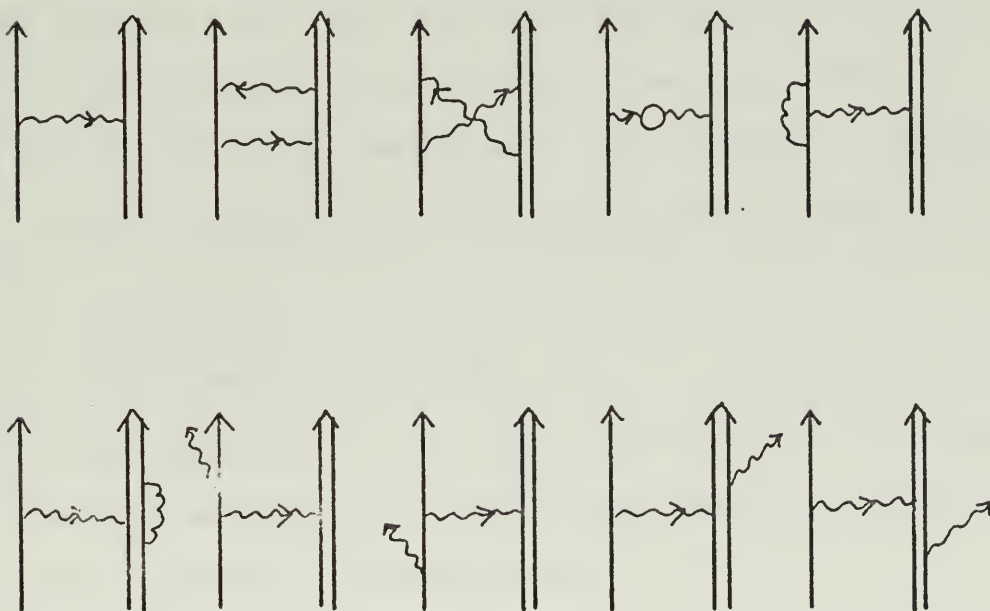

Fig. 5. Feynman diagrams corresponding to the formulas of Meister and yennie and Tsai.

21

Since this calculation was made for potential scattering, the energy of the final and the incident electrons are the same, and the formula is ambiguous as to the energies to use and the definition of ΔE. If we neglect all energy losses except recoil, the most probable energy of the elastically scattered electrons is

$$E_3 = E_1/\eta \qquad\qquad (3\text{-}2)$$

where η is the recoil factor

$$\eta = 1 + E_1 M^{-1}(1-\cos\,\Theta). \qquad\qquad (3\text{-}3)$$

It can be shown that the maximum energy of a photon emitted in the direction of the scattered electron is ΔE, while in the direction of the incident electron the maximum energy is $\eta^2 \Delta E$. To account for this Tsai [13] gives an improved formula:

$$\delta_S = \frac{2\alpha}{\pi}\left\{\left(\frac{1}{2}\ell n\frac{E_1}{\eta^2 \Delta E} + \frac{1}{2}\,\ell n\,\frac{E_3}{\Delta E} - \frac{13}{12}\right)\left[\ell n\left(\frac{-q^2}{m^2}\right) - 1\right] + \frac{17}{36}\right\}. \qquad (3\text{-}4)$$

Note that when $\Delta E \to 0$ all of the above equations are infinite, although we would expect the measured cross section to go to zero as $\Delta E \to 0$. This is apparently due to the fact that multiple photon emissions have been neglected. Hence Schwinger suggested that $(1 - \delta_S)$ be replaced by $e^{-\delta_S}$. It was later proved [15] that the term

$$\frac{2\alpha}{\pi}\left[\ell n\left(\frac{-q^2}{m^2}\right) - 1\right]\ell n\,(\frac{E}{\Delta E})$$

should be exponentiated. It is still uncertain [16] if the other terms should be exponentiated, but the difference is negligible at energies obtainable at the NPGLINAC.

22

Meister and Yennie [16] give an improved version of the Schwinger correction:

$$\delta_S = \frac{\alpha}{\pi}\left\{\left[\ell n\left(\frac{2P_1 P_3}{m^2}\right) -1\right]\ell n\left[\eta\left(\frac{\Delta E}{E_3}\right)^2\right] + \frac{13}{6}\ell n\left(\frac{2P_1 P_3}{m^2}\right) - \frac{1}{2}\ell n^2\eta - \frac{28}{9}\right\}$$

$$+ \frac{Z\alpha}{\pi}\left\{\ell n\,\eta\,\ell n\left[\eta\left(\frac{E_1}{E_4}\right)^2\left(\frac{\Delta E}{E_3}\right)^4\right] - \beta\left(\frac{2E_1}{m}\right) + \beta\left(\frac{2E_3}{m}\right)\right\}$$

$$+ \frac{z^2\alpha}{\pi}\left\{\left[\frac{E_4}{P_4}\ell n\left(\frac{E_4+P_4}{m}\right) -1\right]\ell n\left[\frac{E_1^2}{mE_4}\left(\frac{\Delta E_3}{E_3}\right)^2\right] + \frac{3}{2}\ell n\left(\frac{2E_4}{m}\right) - \frac{1}{2}\ell n^2\left(\frac{E_4}{m}\right)\right\} \quad (3-5)$$

where β is the step function: $\beta(x) = \ell n(x)\theta(1-x)$.

This calculation is described by the Feynman diagrams in Fig. 5. The detailed assumption and restrictions for this calculation are given by Breuer [17], and are similar to those of the Schwinger calculation.

The latest and most accurate version of the Schwinger correction is given by Tsai [18]. This is essentially the Meister and Yennie formula without approximations for the Spence functions. This formula takes into account both target recoil and a dynamical effect due to photon emission. Two-photon emission still has not been sufficiently extracted except in order to cancel infrared divergence in real photon emission. The assumptions, restrictions and Feynman diagrams are the same for the Tsai formulation as for the Meister and Yennie formula. Tsai's expression for the correction is:

$$\delta = \frac{-\alpha}{\pi}\left(\frac{28}{9} - \frac{13}{6}\ln\left(\frac{-q^2}{m^2}\right) + \left(\ln\frac{-q^2}{m^2} - 1 + 2z\ln\eta\right)\left(2\ln\frac{E_1}{\Delta E} - 3\ln\eta\right) - \Phi\left(\frac{E_3-E_1}{E_3}\right) - z^2\ln\frac{E_4}{M}\right.$$

$$+z^2\ln\frac{M}{\eta\Delta E}\left(\frac{1}{\beta_4}\ln\frac{1+\beta_4}{1-\beta_4} - 2\right) + \frac{z^2}{\beta_4}\left\{\frac{1}{2}\ln\frac{1+\beta_4}{1-\beta_4}\ln\frac{E_4+M}{2M} - \Phi\left[-\left(\frac{E_4-M}{E_4+M}\right)^{\frac{1}{2}}\left(\frac{1+\beta_4}{1-\beta_4}\right)^{\frac{1}{2}}\right]\right\}$$

$$+z\left[\Phi\left(-\frac{M-E_3}{E_1}\right) - \Phi\left(\frac{M(M-E_3)}{2E_3E_4-ME_1}\right) + \Phi\left(\frac{2E_3(M-E_3)}{2E_3E_4-ME_1}\right) + \ln\left|\frac{2E_3E_4-ME_1}{E_1(M-2E_3)}\right|\ln\left(\frac{M}{2E_3}\right)\right]$$

$$-z\left[\Phi\left(-\frac{E_4-E_3}{E_3}\right) - \Phi\left(\frac{M(E_4-E_3)}{2E_1E_3-ME_3}\right) + \Phi\left(\frac{2E_1(E_4-E_3)}{2E_1E_4-ME_3}\right) + \ln\left|\frac{2E_1E_4-ME_3}{E_3(M-2E_1)}\right|\ln\left(\frac{M}{2E_1}\right)\right]$$

$$-z\left[\Phi\left(-\frac{M-E_1}{E_1}\right) - \Phi\left(\frac{M-E_1}{E_1}\right) + \Phi\left(\frac{2(M-E_1)}{M}\right) + \ln\left|\frac{M}{2E_1-M}\right|\ln\left(\frac{M}{2E_1}\right)\right]$$

$$+z\left[\Phi\left(-\frac{M-E_3}{E_3}\right) - \Phi\left(\frac{M-E_3}{E_3}\right) + \Phi\left(\frac{2(M-E_3)}{M}\right) + \ln\left|\frac{M}{2E_3-M}\right|\ln\left(\frac{M}{2E_3}\right)\right]\right)$$

$$-\frac{\alpha}{\pi}\left(-\Phi\left(\frac{E_1-E_3}{E_1}\right) + \frac{z^2}{\beta_4}\left\{\Phi\left[\left(\frac{E_4-M}{E_4+M}\right)^{\frac{1}{2}}\left(\frac{1-\beta_4}{1+\beta_4}\right)^{\frac{1}{2}}\right] - \Phi\left[\left(\frac{E_4-M}{E_4+M}\right)^{\frac{1}{2}}\right] + \Phi\left[-\left(\frac{E_4-M}{E_4+M}\right)^{\frac{1}{2}}\right]\right\}\right).$$

(3-6)

B. BETHE-HEITLER CORRECTION

The Bethe-Heitler correction accounts for energy loss by bremsstrahlung in the field of nuclei other than the target nucleus, as well as bremsstrahlung in the field of atomic electrons. A review of bremsstrahlung, screening, and the resulting cross-section formulas is given in Appendix A.

Bethe and Heitler [19,20,21] have shown that if the cross-section for bremsstrahlung were given by

$$\frac{d\sigma}{d\Omega} = \frac{A}{\ln 2\, X_oN}\left[E_1\ln(E_1/E)\right]^{-1},$$

(3-7)

the probability an electron of initial energy E_1 being in an
energy interval dE at E, after traveling through a target of
thickness T (in units of radiation length), would be

$$I_e(E_1 E\ T) = \frac{E_1^{-1}[\ln(E_2/E)]^{T/\ln 2}}{\Gamma(T/\ln 2)} \quad . \tag{3-8}$$

Integration of this formula, with the assumption that T is small,
leads to the original Bethe-Heitler correction, first given by
Hofstadter as

$$\delta_B = \frac{T}{\ln 2}\ \ln\frac{E}{\Delta E}\ \ .$$

To include the effect of target recoil, this should be written

$$\delta_B = -\frac{T}{\ln 2}\ \ \ln\frac{E_1}{\Delta E\,\eta^{\ 3/2}} \quad . \tag{3-9}$$

Bethe and Heitler admit that Eq. (3-7) is a poor approximation
to the correct cross section and was chosen for its simplicity.
To improve upon the correction it is necessary to use a more nearly
correct expression for the cross-section. However, it is also
necessary to be able to perform the integrations.

Tsai [18] has developed a unique method for the case of
complete screening. By combining Eq. (3-7) and Eq. (3-8) for
the case of small T, Eq. (3-8) becomes

$$I_e(E_1,E,T) = \left(\frac{N}{A}\ X_o T\ \frac{d\sigma}{dE}\right)\left(\ln\frac{E_1}{E}\right)^{T/\ln 2} . \tag{3-10}$$

Tsai shows that the term $(\ln E_1/E)^{T/\ln 2}$ is a correction for
multiple scattering which is insensitive to the choice of the
cross-section formula. Hence it would seem appropriate to replace

$d\sigma/dE$ in Eq. (3-10) by a correct expression, thereby immediately obtaining the intensity I_e. By adding the exact cross sections for nuclear and atomic electron bremsstrahlung, the total cross section for one-photon emission and complete screening can be written (with a cross term of $< 0.5\%$ deleted)

$$\frac{d\sigma}{dE} = \left(\frac{d\sigma}{dE}\right)_{nuc} + \left(\frac{d\sigma}{dE}\right)_{elec}$$

$$= X_o^{-1} \frac{A}{N} \frac{4}{3} \left(E_1-E\right)^{-1} \left[\frac{E}{E_1} + \frac{3}{4}\left(\frac{E_1-E}{E_1}\right)^2\right]\left[1 + \frac{E}{9E_1}\frac{Z+1}{Z+\xi}\left[\ln\left(183Z^{-\frac{1}{3}}\right)\right]^{-1}\right],$$

where X_o is the radiation length given by Bethe and Ashkin [22]

$$\frac{1}{X_o} = \left(\frac{4N}{A}\right)\alpha r_o^2 Z(Z + \xi)\ \ell n\left(183Z^{-\frac{1}{3}}\right).$$

Thus Eq. (3-8) becomes

$$I_e(E_1,E,T) = bT(E_1-E)^{-1}\left[\frac{E}{E_1} + \frac{3}{4}\left(\frac{E_1-E}{E_o}\right)^2\right]\left(\ell n\ \frac{E_1}{E}\right)^{bT}, \qquad (3-12)$$

where to a very good approximation

$$b = \frac{4}{3}\left\{1 + \frac{1}{9}\left[(Z+1)/(Z+\xi)\right]\left[\ell n\left(183Z^{-\frac{1}{3}}\right)\right]^{-1}\right\}, \qquad (3-13)$$

and ξ is the Wheeler-Lamb factor.

From this, Tsai evaluates the correction under the assumption that the scattering event occurs midway through the target. He also incorporates energy loss in an entrance window of thickness T_{iw} and a final window of thickness T_{fw} to derive the formula

$$\delta_B = \left\{\left[b_w T_{iw} + \frac{1}{2}\ bT\right]\ell n(E_1/\eta^2\Delta E) + \left[b_w T_{fw} + \frac{1}{2}\ bT\right]\ell n(E_3/\Delta E)\right\}. \qquad (3-14)$$

In examining, for example, the proton scattering in a solid target such as $(CH_2)_n$, bremsstrahlung from the carbon in the target can be accounted for by substituting the effective thickness of the carbon for the window thickness.

The expression for δ_B as derived by Tsai is slightly more accurate than Eq. (3-9) and certainly more versatile. It is, however, derived on the assumption of complete screening, an approximation which begins to fail at energies attainable by the NPGLINAC. Unfortunately, the magnitude of the errors induced is, as yet, unknown. A more correct theory would require use of a cross-section formula which includes the effects of "intermediate" screening. These formulas, which include atomic form factors, are not known explicitly and determination of the correction would require a double numerical integration, with no hope of an explicit expression for the Bethe-Heitler correction[2]. There was insufficient time to pursue this idea further for inclusion in this paper.

───────────

[2]Incorporating the effects due to screening also means re-evaluating the Wheeler-Lamb factor which in turn implies changes in the radiation length.

IV. CHOICE OF ΔE

The shape of an elastic spectrum near the peak is largely due to the energy spread of the incident electron beam. A broadening of the peak is also due to the finite width of the entrance slit as well as the ionization and radiative corrections. The corrections should be able to account for electrons lost by ionization and by radiation for any reasonable choice of ΔE. However ΔE must be chosen sufficiently large to include the energy spread due to the two machine effects.

Tsai [13] gives requirements on the choice of ΔE. If the incident beam has an energy spread of ΔE_1, the equation

$$E_3 = E_1/\eta$$

is used to calculate the energy spread of the scattered electrons:

$$\left(\frac{\delta E_3}{\delta E_1}\right) \Delta E_1 = \Delta E_1 \eta^{-2} \ .$$

η is the recoil factor given in Eq. (3-3). Similarly Tsai shows that the energy spread due to the finite width of the entrance slit is

$$\left(\frac{\delta E_3}{\delta \Theta}\right) \Delta \Theta = \left(\frac{E_1^2}{M\eta^2}\right) \sin \Theta d\Theta.$$

Hence ΔE should be chosen such that

$$\Delta E >> \Delta E_1 \eta^{-2},$$

and

$$\Delta E > (E_3^2 / M) \sin \Theta \Delta \Theta.$$

28

In the development of the Tsai formulation of the Schwinger correction there is an assumption

$$E(1 + 2E_1/M) \ll E_3.$$

This puts an upper limit on the choice of ΔE, but is not a severe restriction.

V. EXPERIMENTAL CONSIDERATIONS

A. COUNTING SYSTEM

The design and operation of the NPGLINAC has been described in detail in several theses [3,4]. The most significant recent modification has been the installation of a ten-channel counting system. Ten plastic scintillators have been positioned vertically in the focal plane of the 16 inch double-focusing spectrometer. The spectrometer is described in a thesis by Oberdier [23].

Electrons which enter the spectrometer with an energy (more properly, momentum) corresponding to a given spectrometer setting follow a path through the spectrometer such that they focus at the intersection of the focal plane and an extension of the central path of the spectrometer. Electrons of greater energy are focused above this point in the focal plane while less energetic electrons are focused at a lower point. The distance from the central point is given roughly by the dispersion formula

$$\delta_a = \left(\frac{\Delta p}{p}\right) \cdot D \cdot r \qquad (5-1)$$

where

r = central radius of the spectrometer = 16 inches

D = dispersion constant = 3.92

$\left(\frac{\Delta p}{p}\right)$ = momentum difference from central focusing point.

The ten scintillators are arranged above and below the central point (channel five very nearly corresponds to the central energy) so that each one "sees" a different energy.

Immediately behind the front counters is a large vertical backing
scintillator. To minimize the detected background due to the
intense radiation field in the accelerator end station, only
electrons which pass through both one of the front counters and
the back counter in coincidence are registered as scattered
electrons. The coincidence system is illustrated schematically
in Fig. 6.

To get a reasonable density of points defining a scattering
peak it is necessary to change the central energy of the spec-
trometer in small steps of one-third to one-sixth the average
counter separation (0.10 to 0.05 MeV at E_1 = 90 MeV), as well as
one or more large steps (~2.5 MeV at E_1 = 90 MeV) to define the
radiation tail. This requires a rather involved data unfolding
procedure before a usable spectrum is produced. We follow
closely the procedure given by Suelzle [24,25]. The energy of
each counter as a function of the central energy has been deter-
mined by plotting, at several incident energies, the elastic
peak as it occurs in each channel as a function of the spectro-
meter setting. The resolution of the i-th channel is defined as

$$E_i = \frac{1}{2} (E_{i+1} - E_{i-1}).$$

The efficiency of each channel is determined for each run by
taking at least five overlapping data sets on a smooth portion of
the radiation tail and fitting these points to a second order poly-
nomial. The efficiency of each channel is then found from the
difference of the data points and the polynomial fit.
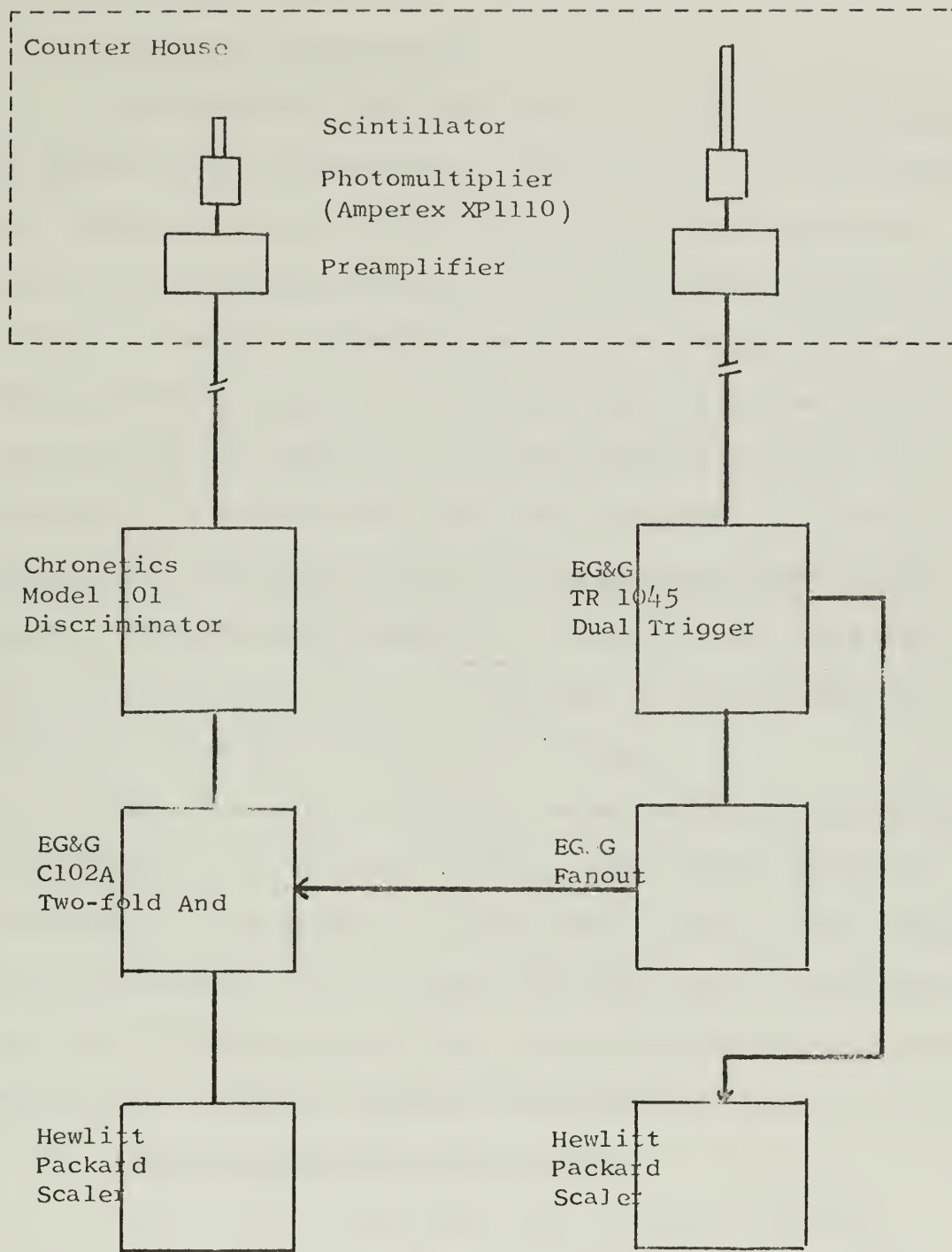
Fig. 6. Counting System

B.   EXPERIMENTAL METHOD

   1.   Basis of the Experiment

      The purpose of this experiment is to examine the adequacy

of the radiative corrections as a function of target thickness, and

the importance of the cutoff energy, E_3, to the corrections.   This

leads to the straight-forward procedure of determining the cross

section for several thicknesses of the same target material at a

given incident energy and scattering angle.   Since we are only

interested in the relative differences between targets, it is

sufficient to determine the area under the peaks.   If the cor-

rections are correct, the ratio of the corrected area to the

target thickness will be constant.   Similarly, for any single peak,

the corrected area should be independent of ΔE, provided the

conditions discussed in Section IV are met.

      These corrections have been examined for six thicknesses

of graphite, $\rho = 1.441$ g/cm^3 (.028 to .250 inches) and seven

thicknesses of aluminum, $\rho = 2.543$ g/cm^3 (.0104 to .1354 inches).

Incident energies of 35, 55 and 90 MeV were used.   The scattering

angle was 90 degrees in all runs.   The dependence of area on ΔE

was examined on several targets at different energies.

   2.   Internal Consistency of the Data

      In this work it was necessary to measure the area

(counts) of an elastic peak but not necessary to actually de-

termine the cross section.   Therefore errors in the measurement

of the absolute values of experimental constants (incident energy,

scattering angle, target angle, solid angle, integrator capacitance, SEM efficiency and others) do not enter into these relative experiments. However, it is important to insure that none of these factors vary during a data run.

To avoid effects which may be due to the tuning of the accelerator, such as variations in incident energy, energy resolution of the beam, and spot size of the beam, it has not been attempted to compare different runs. A run, consisting of a spectrum from each target, was completed without retuning the beam. It is felt that the deflection magnets, which define the incident energy, drift less than 0.1% over several hours, while short term variations are undetectable.

To avoid errors due to hysteresis in the spectrometer, the magnet current, and hence the central energy, is monotonically decreased during the run to span the peaks. Because of drift in the current regulated supply or temperature change in the magnet, the field of the magnet is not exactly proportional to the current in the windings. Hence the field is sensed by a rotating-coil fluxmeter, and maintained at a specified value by a balancing circuit. The field is held constant to approximately $\pm .005$ MeV in the central energy. The precision potentiometer used in the balancing circuit to define the field value is linear to 0.1% throughout its range.

It is critical that the SEM efficiency and its associated beam current integrator be constant over the time of the experiment. Since the beam intensity must vary during a run to account

for the difference in target thickness, the efficiency of the SEM must be independent of beam current, or a correction must be known. This is fully discussed in Appendix B.

There is some question as to the validity of the efficiency determination for the individual counters. To minimize such errors, all peaks have been taken so that the top of the peak is defined entirely by channel seven. Thus the efficiencies, even if incorrect by several percent, are applied similarly to all peaks.

With the previous one-channel system it was determined that a counting rate correction of the form

$$C_T = C[1.0 + 0.003C/t]$$

where

C_T = corrected counts

C = observed counts

t = integration time in seconds

should be applied to the observed counting data. This same correction has been applied to data taken on the ten-channel system, although it is now apparent that this is too large. However, roughly the same counting rate, ten counts per second, was maintained when running each peak, so that errors will again cancel out. It is estimated that accidental coincidences do not contribute more than a 0.1% error to the cross sections.

The most persistent problem encountered during this experiment was the detection of an excessive number of electrons in the upper channels when counting on a radiation tail. This problem was partially solved by simply deleting obviously bad points before the numerical integration of the peak. A discussion of this problem ill be found in Appendix C.

VI. DATA ANALYSIS

A. DETERMINATION OF CROSS SECTION

The data from an electron scattering experiment is in the form of a counts versus MeV (properly MeV/c) spectrum of the scattered electrons. This spectrum is unfolded from the raw data by the procedure mentioned in Section V. To find the actual number of scattered electrons it is necessary to first divide out the momentum acceptance of each counter, Δp. To a very good approximation this is given by the dispersion formula

$$\Delta p = \frac{a/r}{D \cdot p} \qquad (6\text{-}1)$$

where now a is the effective height of each counter, approximately 7/32 inch. The resulting spectrum is thus one of counts per MeV versus MeV, so that if the area of the peak is measured it has units of counts, the number of scattered electrons. The number of scattered electrons per millivolt integration of the incident beam is proportional to the cross section.

Determination of the area was by numerical integration of the unfolded spectrum. A three-point method, similar to Simpson's Rule, was chosen. Since the data points were not equally spaced, it was necessary to exactly fit each set of three points to a parabola, and to explicity perform the integration under the curve. It is felt that this method is superior to the commonly used trapezoidal rule.

Once the areas have been determined, it is a simple procedure to apply the corrections and normalize the areas to a given target thickness. All the corrections except the most complicated

36

of the Schwinger corrections, Eq. (3-6), lend themselves to computation by hand or with a calculator.

The data is presented in two forms. To examine the validity of the Bethe-Heitler correction the ratio of the corrected area to the target thickness versus target thickness has been plotted for each run. Straight line least squares fits have been included. To examine the choice of ΔE, the corrected area versus ΔE has been graphed for several targets at different energies.

B.   EXPERIMENTAL ERROR

The statistical error in the cross section due to the random nature of scattering reactions is very nearly

$$\sigma = \frac{\sqrt{\Sigma n_i}}{\Sigma n_i}$$

where σ is the standard deviation and Σn_i is the total number of counts in a peak. Typical statistical uncertainties vary from one-half of one percent to one percent for the experiments reported in this paper.

A significant contribution to the uncertainty of the measured cross section is introduced by the numerical integration. By adding or deleting points on a peak and repeating the integration, this uncertainty has been estimated to be about one percent (slightly greater for the thin targets which have fewer points defining the peak and slightly less for the thick targets).

The target thickness is known to one percent (with smaller errors for the thicker targets). For the experiments which compare the cross section as a function of target thickness, these errors propagate to a total uncertainty of about 1.5%. Experiments to determine the proper choice of ΔE are not subject to these uncertainties since only one peak is integrated, and the successive integrations over the peak are performed only with variations in the lower cutoff energy. The relative uncertainty in these successive integrations is estimated to be less than one-half of one percent.

Because of the relative nature of all the experiments, systematic errors are thought to be insignificant.

VII. RESULTS

A. CHOICE OF ΔE

The data from the experiments to determine the appropriate choice of ΔE are shown in Figs. 7 to 13, and summarized in Table II. Figure 7 is a plot of the cross section versus ΔE for carbon data taken on the Mark III linear accelerator at Stanford University [26]. The cross section does not approach an symptotic value even for a ΔE of 20 half-widths[3]. Figures 8 to 13 show typical experimental results obtained with the NPGLINAC. In almost all cases an syn totic value was reached for a ΔE of four half-widths (six half-widths in the worst case, $E_1 = 35.0$ MeV). No significant difference was noted when the energy defining slits were opened from the normal position of .0920 inches to .1840 inches, although the resolution[4] of the incident beam, $\Delta E_1/E_1$, changed from 0.4% to 0.8%. Note that these values are less than two half-widths of the elastic peak, so that this is the expected result.

---

[3]Cross sections were calculated by the procedure outlined for the NPGLINAC; however, Bumiller and Dally [26] report similar results using the same data.

[4]$\Delta E_1/E_1 = x/r_o$
x = opening of the slits in inches
r_o = effective radius of the deflection magnet, 23 inches

TABLE II.

Representative Data to Determine Choice of ΔE

RUN NO.	TARGET	THICKNESS (INCHES)	E_1	FIGURE NO.	COMMENTS
0051	Carbon	.055	117.4	7	data from Bumiller and Dally (HEPL)
1021	Carbon	.0282	90.0	8	
1261	Aluminum	.0104	90.0	9	
1064	Carbon	.1118	90.0	10	
1270	Aluminum	.0315	90.0	11	slits = 100.0 (.0920 inches)
1273	Aluminum	.0315	90.0	12	slits = 200.0 (.1840 inches)
1281	Aluminum	.0104	35.0	13	

Fig. 7.
Run 51
E_1 = 117.4
Carbon

typical
error

$d\sigma/d\Omega \longrightarrow$

ΔE
(half-widths)
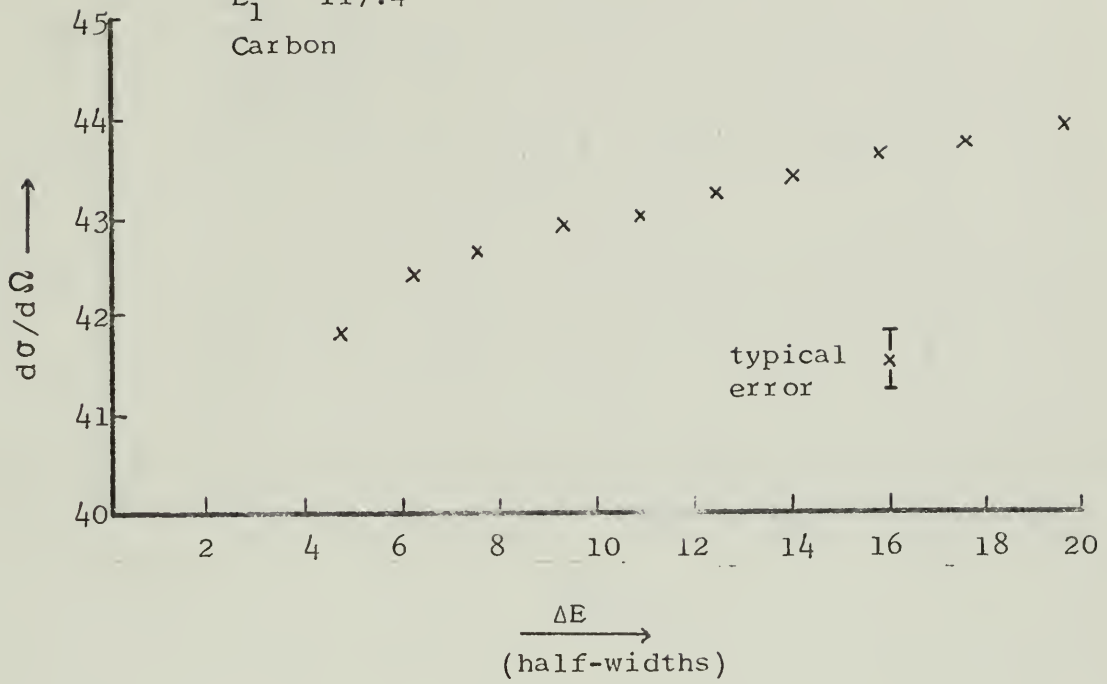
Fig. 8.
Run 1021
E_1 = 35.0
Carbon

$d\sigma/d\Omega \longrightarrow$

ΔE
(half-widths)

41

Fig. 9.
Run 1261
E_1 = 90.0 MeV
Aluminum

Fig. 10.
Run 1264
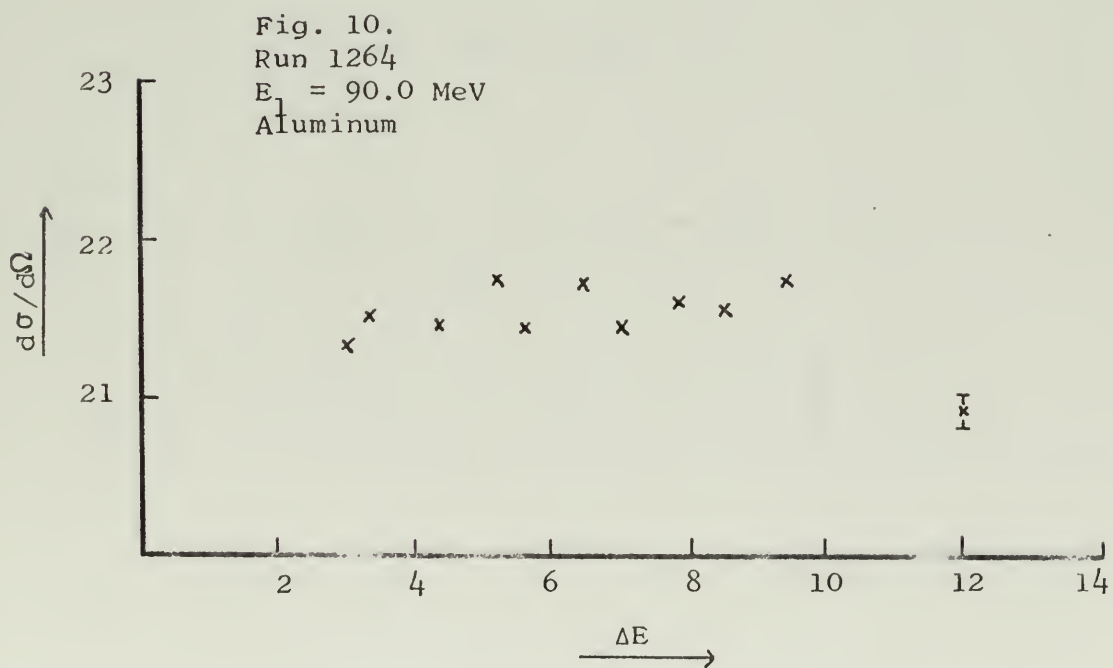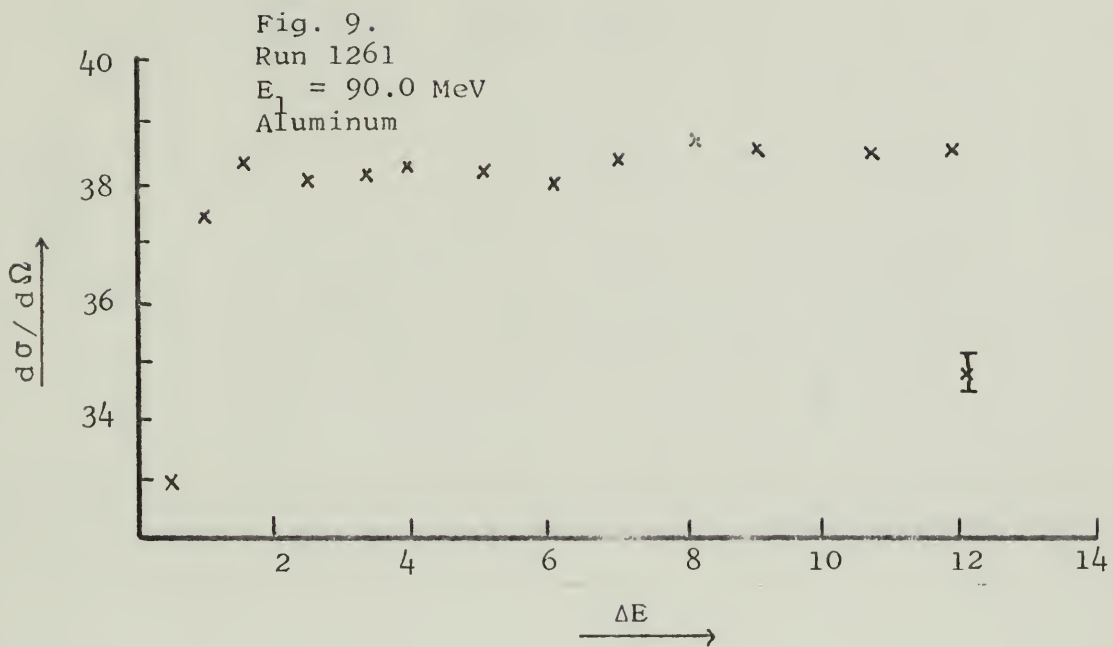E_1 = 90.0 MeV
Aluminum
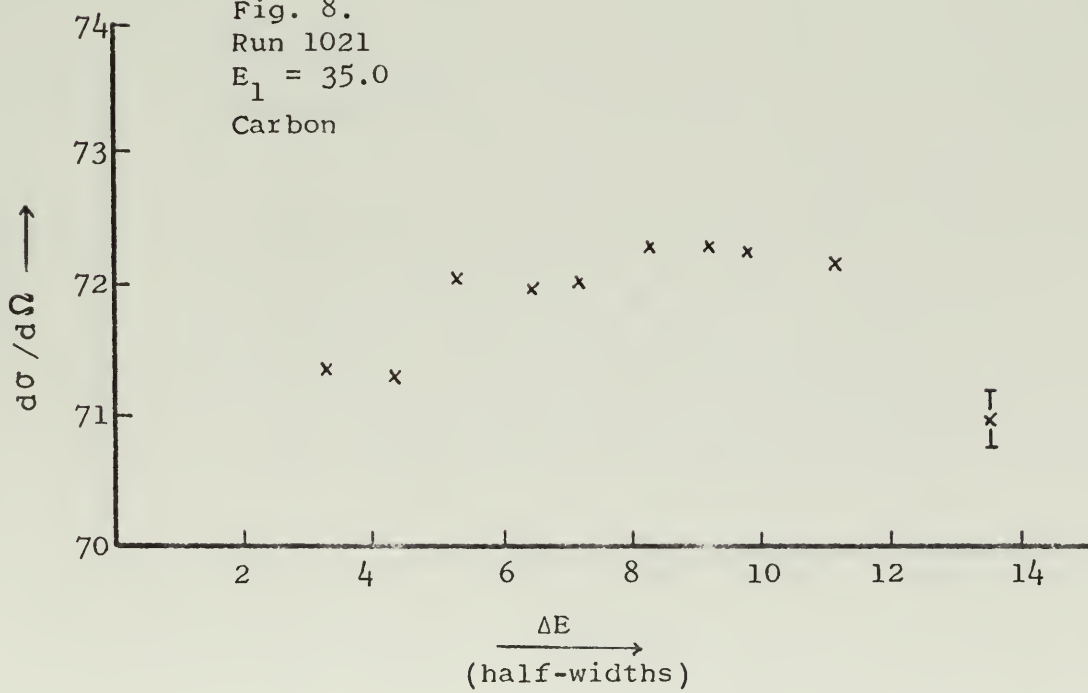
Fig. 11.
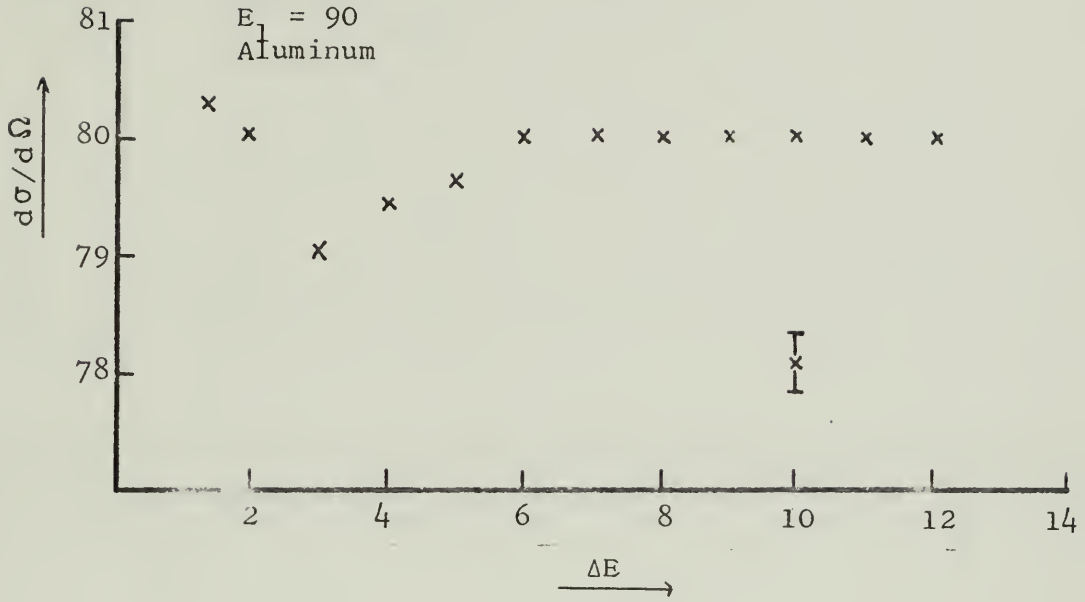Run 1270   slits = 100.
E_1 = 90
Aluminum

Fig. 12.
Run 1270   slits = 200.
E_1 = 90
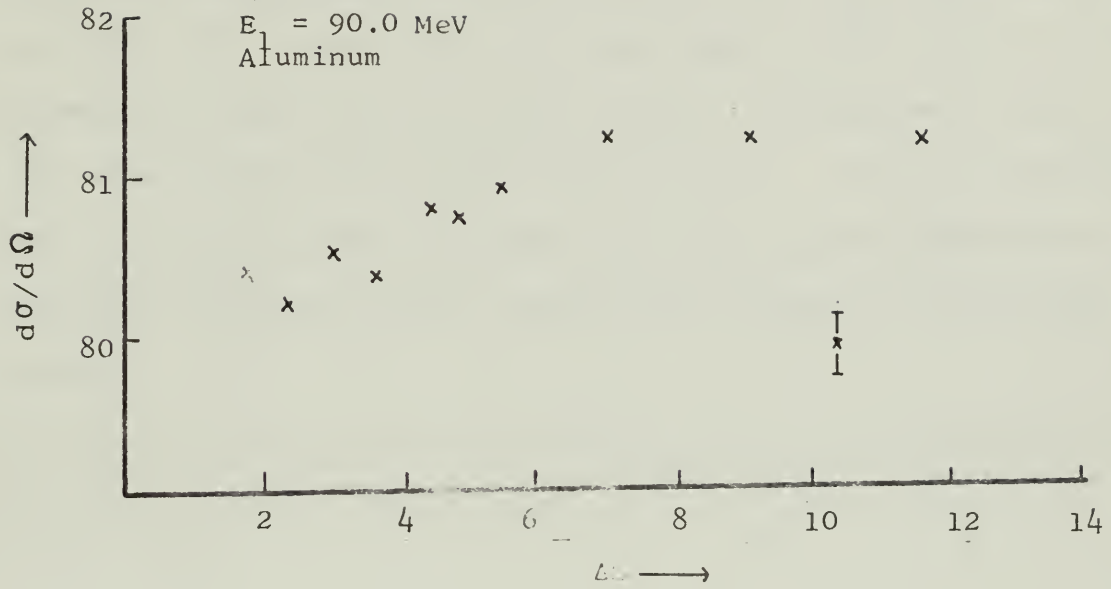Aluminum

43
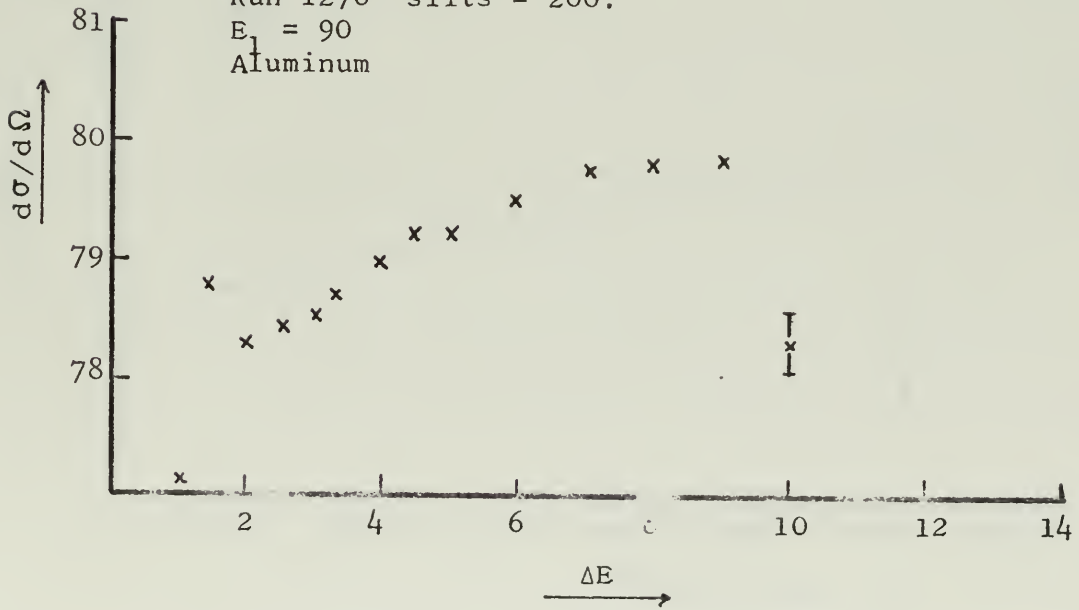
Fig. 13.
Run 1281
$E_1 = 90.0$ MeV
Aluminum

Fig. 14.
Run 1030
$E_1 = 90.0$
Carbon

thickness (x_o) ⟶

44
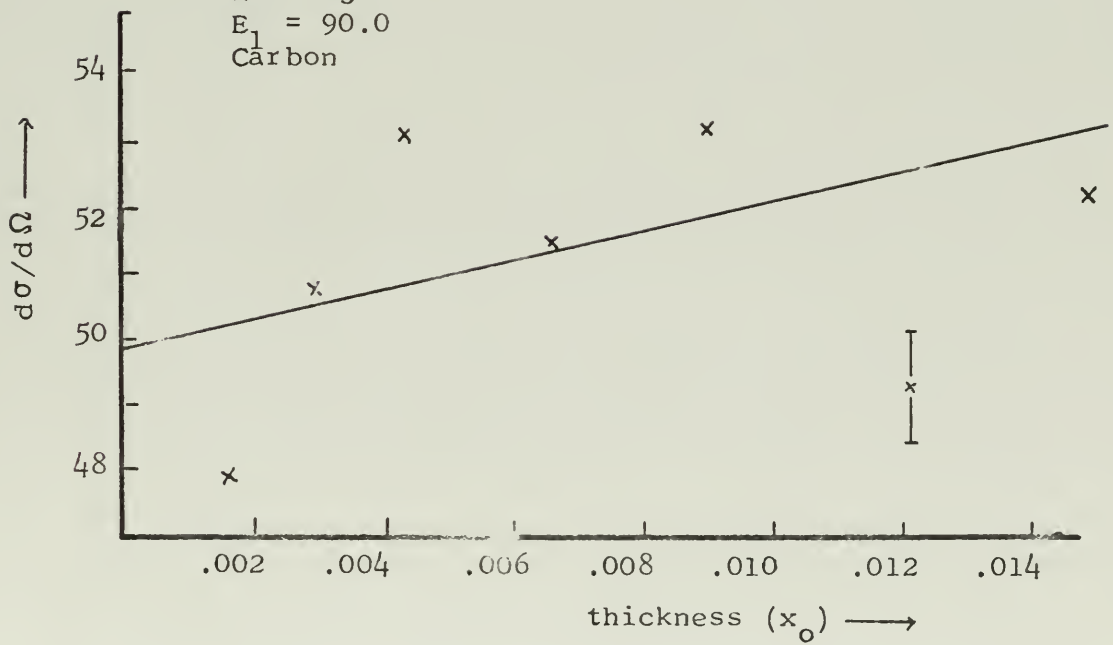
B. ACCURACY OF THE CORRECTIONS

The data from the experiments to determine the validity of the corrections to the cross section are shown in plots of cross section versus target thickness in Figs. 14 to 22, and summarized in Table III. In all cases the experimental cross section is considerably larger for the thicker targets. No systematic errors are known which could account for this fact. In fact, the possible errors, change in SEM efficiency with beam current (APPENDIX B) or multiple scattering events, would tend to magnify the observed effect.

TABLE III.

Summary of Data, Cross Section as a Function of Thickness

RUN NO.	TARGET	E_1	%CHANGE IN* CROSS-SECTION	$\Gamma^{\dagger}$	FIGURE NO.
1030	Carbon	90.0	4.4	4	14
1041	Carbon	55.55	6.5	4	15
1060	Carbon	90.0	1.2	6	16
1220	Aluminum	35.0	10.5	4	17
1280	Aluminum	35.0	14.0	4	18
1230	Aluminum	90.0	7.8	4	19
1240	Aluminum	90.0	6.6	4	20
1260	Aluminum	90.0	7.8	4	21
1260	Aluminum	90.0	8.2	7	22

* % change in cross section from zero thickness target to thickness of .01 radiation lengths.

† Γ = number of half-widths for integration.
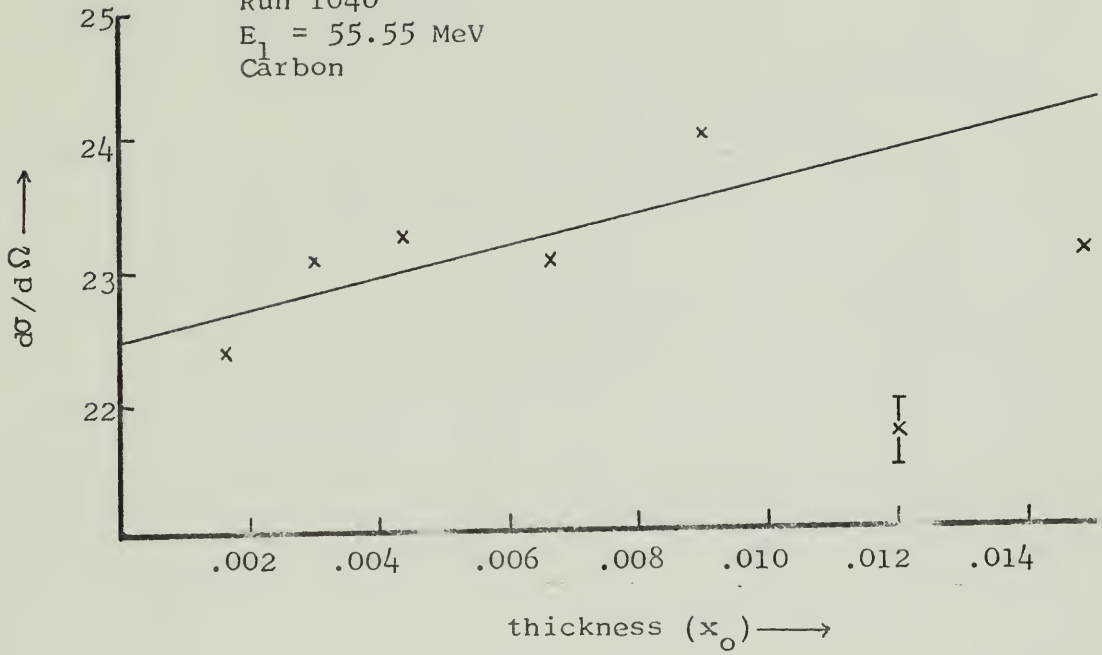
46

Fig. 15.
Run 1040
E_1 = 55.55 MeV
Carbon

thickness (x_o) ⟶

Fig. 16.
Run 1060
E_1 = 90.0 MeV
Carbon

thickness (x_o) ⟶

Fig. 17.
Run 1220
$E_1 = 35.0$ MeV
Aluminum

$d\sigma/d\Omega \longrightarrow$

thickness $(x_o) \longrightarrow$

Fig. 18.
Run 1280
$E_1 = 90.0$ MeV
Aluminum

$d\sigma/d\Omega \longrightarrow$

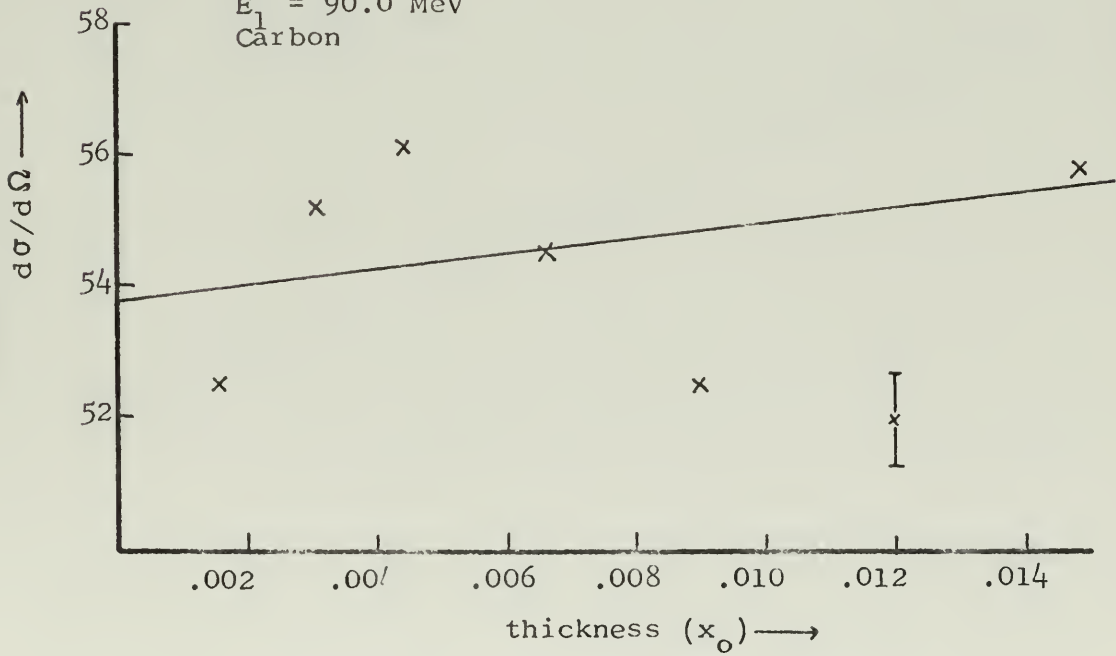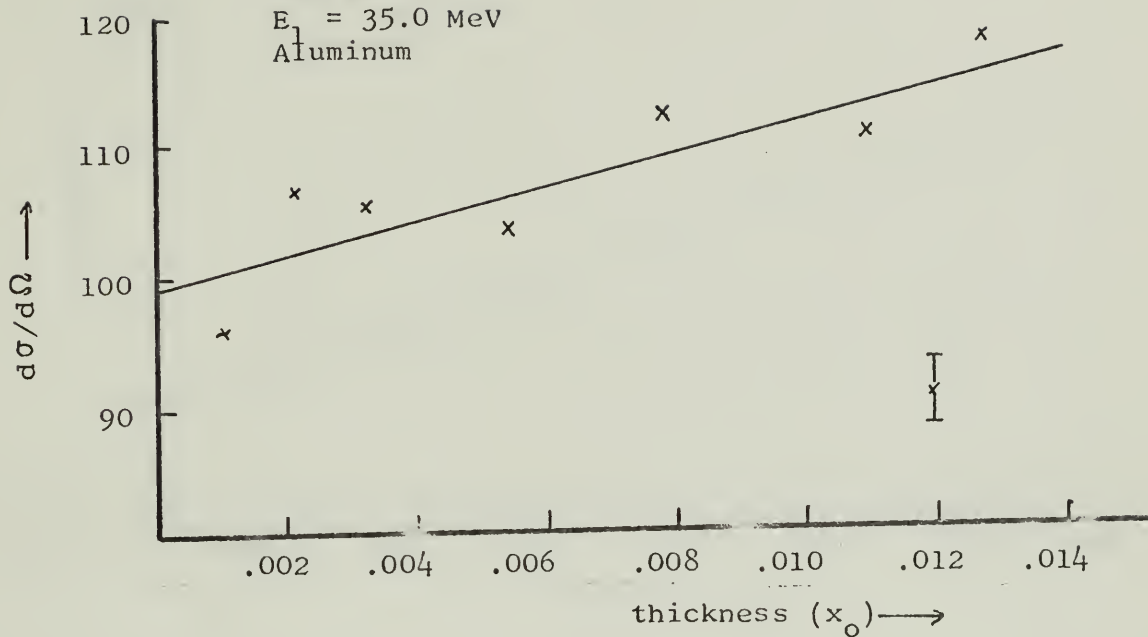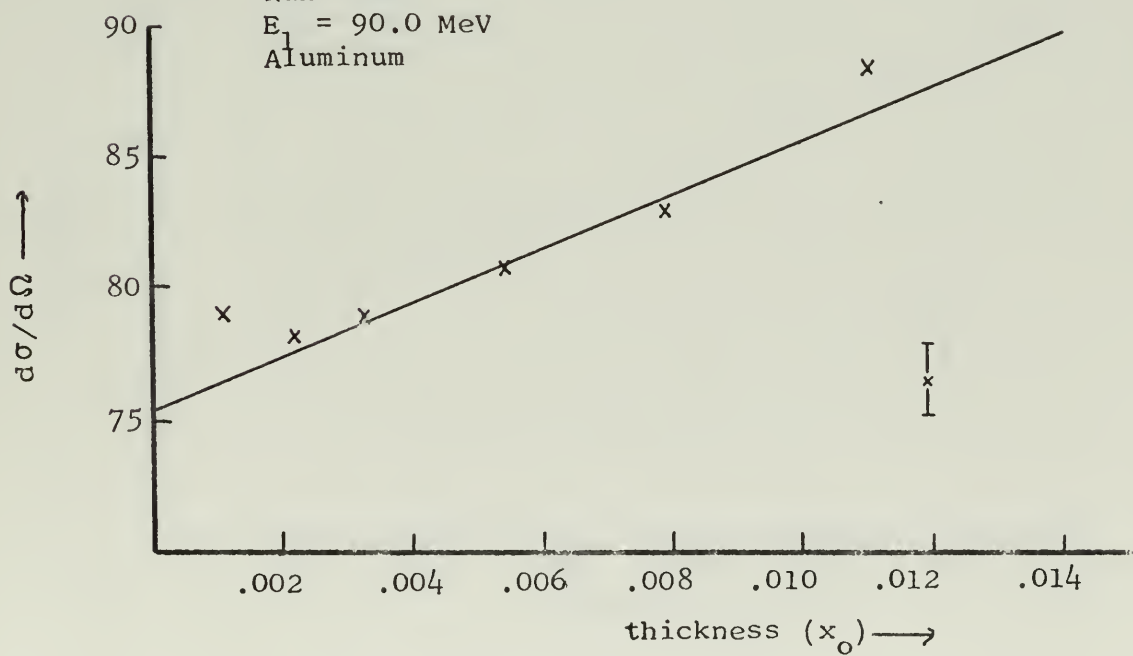thickness $(x_o) \longrightarrow$

Fig. 19.
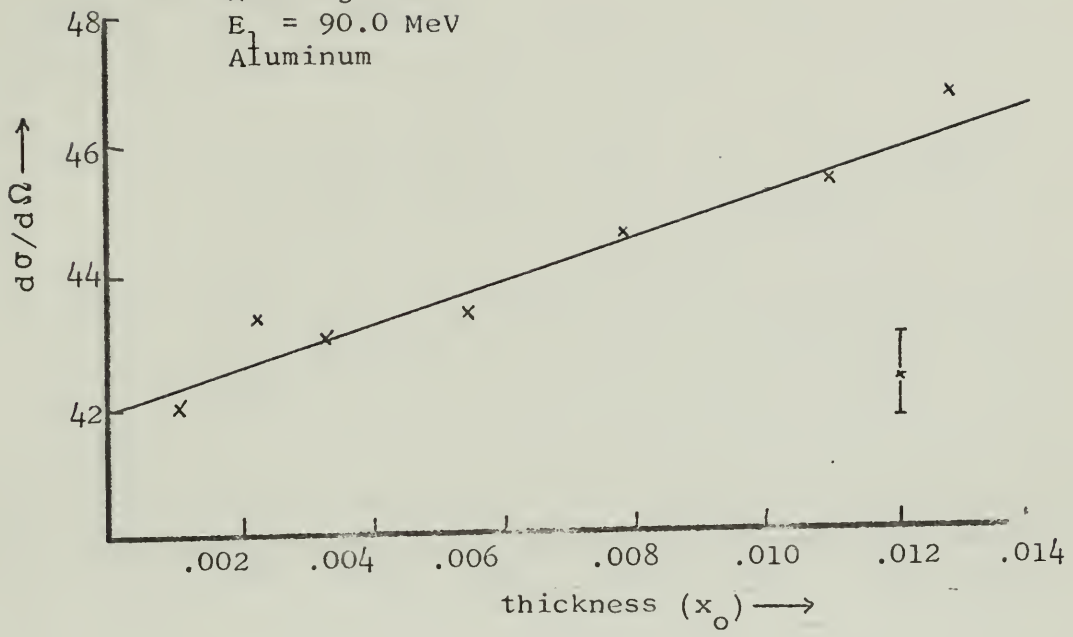Run 1230
E_1 = 90.0 MeV
Aluminum

Fig. 20.
Run 1240
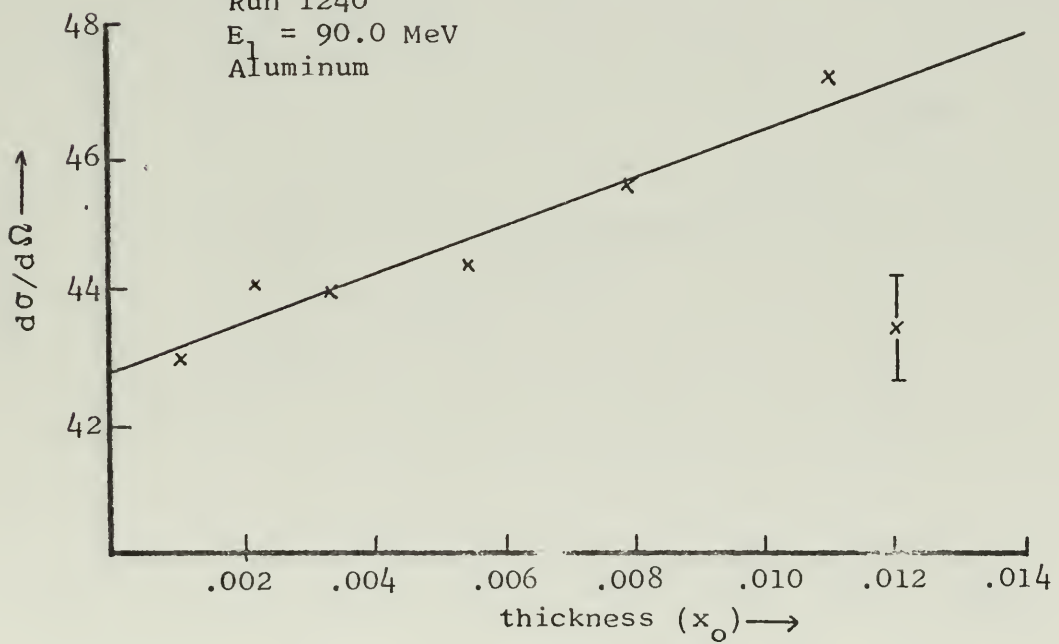E_1 = 90.0 MeV
Aluminum

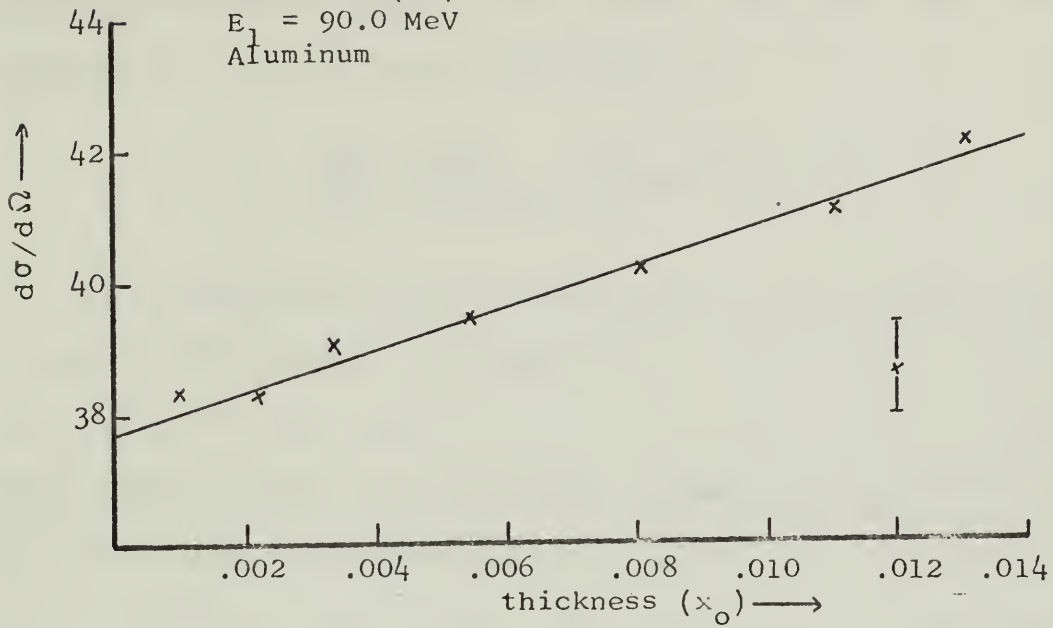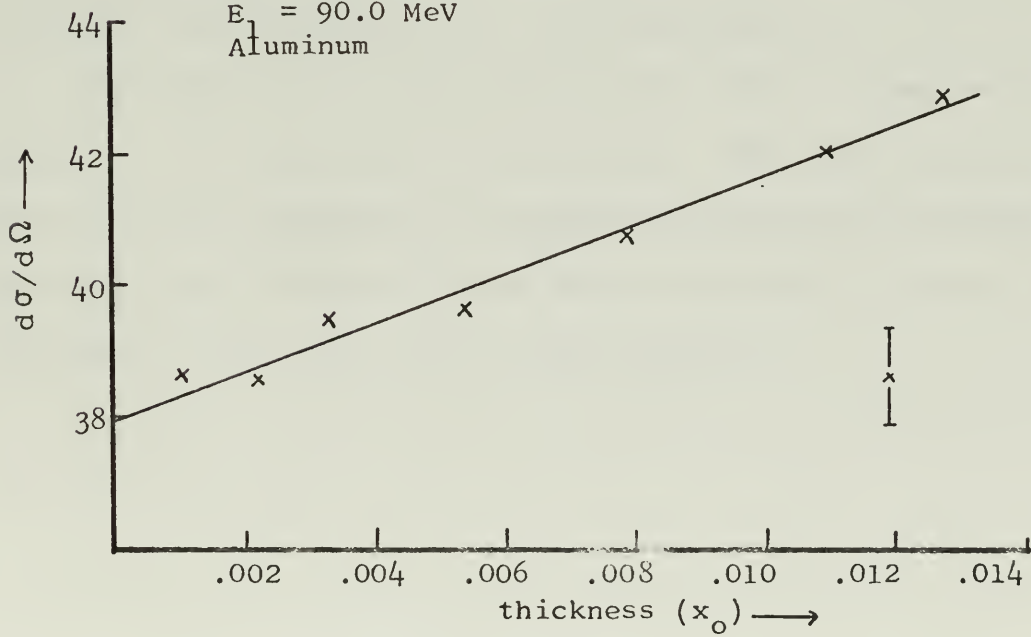Fig. 21.
Run 1260 (4Γ)
E_1 = 90.0 MeV
Aluminum

Fig. 22.
Run 1260 (7Γ)
E_1 = 90.0 MeV
Aluminum

VIII. CONCLUSIONS

The ionization and radiative corrections are most accurately
given by Equations (2-3), (3-6), (3-14). Thus the cross section as
determined by a scattering experiment is

$$\frac{d\sigma}{d\Omega} = \left(\frac{d\sigma}{d\Omega}\right)_{exp} = K_b^{-1} \exp\left[\delta_s + \delta_b\right] \quad .$$

By integrating the experimental spectra for several successively
lower cut-off energies and applying the corrections, it was deter-
mined, within experimental error, that a ΔE of four half-widths is
more than adequate, even for thick targets (0.01 radiation lengths)
even with the energy defining slits opened more than usual
(slits = 200. = .184 inches). The consistency of this data in-
dicates that the unfolding procedure and the numerical integration
was done properly. Data taken on the Mark III accelerator does
not converge even when the integration is carried out to 20 half-
widths. This discrepancy has not been explained.

For thick targets these corrections lead to cross sections
which are too large by several percent. This may be due to the
fact that the assumption of complete screening in the Bethe-
Heitler theory begins to break down at energies in use at the
NPGLINAC. This error has not been estimated.

APPENDIX A. BREMSSTRAHLUNG

A complete theory of bremsstrahlung has been developed by Bethe and Heitler [19,20,21]. Other authors have developed similar theories, but they lead to essentially the same results. Since knowledge of the bremsstrahlung cross sections is basic to the Bethe-Heitler radiation correction, it is appropriate to review the basic features of the Bethe-Heitler theory.

When an electron of initial energy E_1 passes through the electromagnetic field of a nucleus, the interaction of the two fields results in an acceleration to the electron so that it must emit radiation. The emission of a quantum of momentum $\vec{k}/c$ leads to a final electron state of energy E:

$$k = h\nu = E_1 - E .$$

The problem is thus to find the transition probability, or cross section to the final state E (momentum $\vec{p}$).

The analysis involves the interaction of the electron with the radiation field[5], H, and the nuclear field[6], V, both of which are treated as perturbations. There are thus two intermediate states, one caused by H where the quantum $\vec{k}$ is emitted, so that the electron has momentum

$$\vec{p}' = \vec{P}_o - \vec{K},$$

and a competing intermediate state caused by V, where the electron has momentum

$$\vec{p}'' = \vec{p} + \vec{K}$$

---

[5] $H = - e\vec{\alpha}\,\vec{A}$, where $\vec{A}$ is the vector potential, $\vec{\alpha}$ the velocity.

[6] Assume a Coulomb field, $V = Ze^2/r$.

and $\vec{k}$ is emitted with conservation of momentum in the transition from intermediate to final states. By appropriately summing over the intermediate states one can determine the matrix elements for the total transition, K_{FO}[7]. This leads directly to the differential cross section[8]. This has been integrated over all angles by Bethe [21] to derive the cross section (differential in energy) for the case of no screening:

$$\frac{d\sigma}{dE} = \frac{z^2 \alpha r_o^2}{[E_1 - E]} \, 4 \left[1 + \left(\frac{E}{E_1} \right)^2 - \frac{2}{3} \frac{E}{E_1} \right] \left(\ell n \frac{2E_1 E}{nc^2 [E_1 - E]} - \frac{1}{2} \right). \quad (A-1)$$

This result was derived on the assumption of a pure Coulomb field, but in certain cases the screening of the nuclear field by the atomic electrons necessitates significant changes. The charge distribution changes the original potential

$$V = \int \exp \frac{[i(\vec{q} \cdot \vec{r})/\hbar c]}{r} \, d\tau = \frac{4 \pi \hbar^2 c^2}{q^2} \, z^2$$

$$V = \frac{4 \pi \hbar^2 c^2}{q^2} \, [z - F(q)]^2$$

where F is the atomic form factor of the Fermi-Thomas model

$$F(q) = \int \rho(r) \exp \left[\frac{i}{\hbar c} \left(\vec{q} \cdot \vec{r} \right) \right] d\tau ,$$

with $\rho(r)$ the density of atomic electrons. Hence screening may be accounted for by replacing z^2 in the original differential cross-section formula by $[z - F(q)]^2$.

---

[7] Equation (25-8) in Reference 20.

[8] Equation (25-13) in Reference 20.

For screening to be significant, the field must be screened appreciably for "impact parameters" which contribute most to the bremsstrahlung process. $F(q)$ becomes comparable to Z for

$$q \leq \frac{mc^2}{137} Z^{1/3} \quad,$$

which is $\hbar c$ times the reciprocal of the atomic radius. It can also be shown that there is a minimum value of q,

$$q_{min} = \frac{(mc^2)^2 h\nu}{2E_1 E} \quad.$$

Then screening is effective if

$$E_1 E / h\nu > \frac{1}{2} \ 137 \ mc^2 \ Z^{-\frac{1}{3}} \quad.$$

Numerical integration over the angles involved by Bethe leads to the general formula

$$\frac{d\sigma}{dE} = \frac{Z^2 \alpha}{E_o^2 (E_o - E)} \left[\left(E_o^2 + E^2 \right) \left(\emptyset_1(\gamma) - \frac{4}{3} \ln Z \right) - \frac{2}{3} E_o E \left(\emptyset_2(\gamma) - \frac{4}{3} \ln Z \right) \right] \quad \text{(A-2)}$$

where

$$\gamma = \frac{100 \ mc^2 \ h\nu}{E_o E \ Z^{\frac{1}{3}}} \quad.$$

$\emptyset_1$, $\emptyset_2$ are given in Fig. 23. γ determines the effect of screening. If $\gamma = 0$ the screening is said to be complete while for $\gamma \gg 1$ screening may be neglected.

In the case of complete screening, Eq. (A-2) reduces to

$$\frac{d\sigma}{dE} = \frac{Z^2 \alpha r_o^2}{[E_1 - E]} \ 4 \left\{ \left[1 + \left(\frac{E}{E_1} \right) - \frac{2}{3} \frac{E}{E_1} \right] \ln \left(183 \ Z^{-\frac{1}{3}} \right) + \frac{1}{9} \frac{E}{E_1} \right\} \quad. \qquad \text{(A-3)}$$

54

Fig. 23.   Influence on Screening by Atomic Electrons (high energy). $\emptyset_1$, $\emptyset_2$ used in Eq. (A-2).
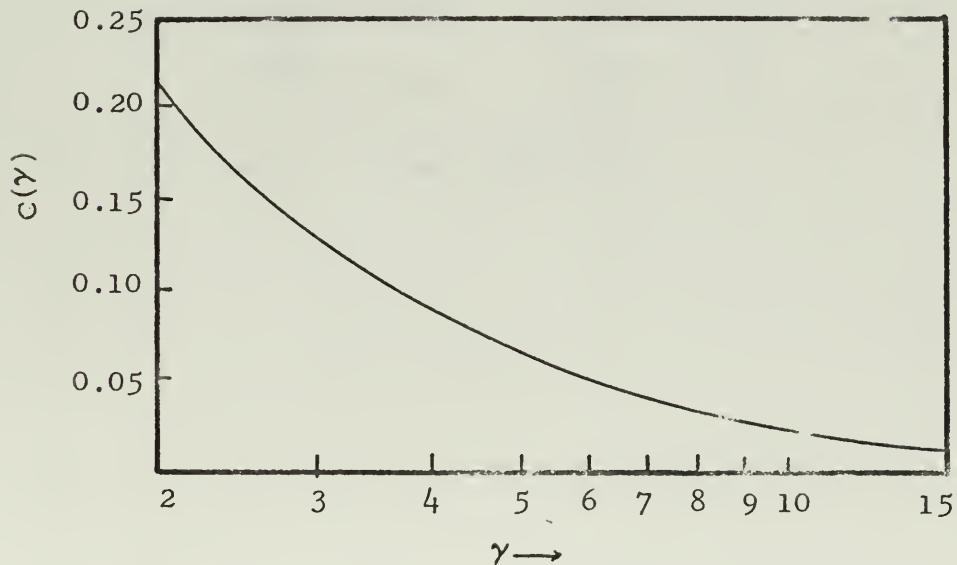
Fig. 24. Influence on Screening by Atomic Electrons (lower energy). $C(\gamma)$ used in Eq. (A-5).

55

Two different expressions may be written for the intermediate cases:

$\gamma < 2$:

$$\frac{d\sigma}{dE} = \frac{z^2 \alpha r_o^2}{[E_1 - E]} \, 4 \left\{ \left(1 + \frac{E^2}{E_1^2}\right) \left[\frac{\emptyset_1(\gamma)}{4} - \frac{1}{3} \ln z\right] - \frac{2}{3} \frac{E}{E_1} \left[\frac{\emptyset_2(\gamma)}{4} - \frac{1}{3} \ln z\right] \right\} \quad (A-4)$$

$2 < \gamma < 15$:

$$\frac{d\sigma}{dE} = \frac{z^2 \alpha r_o^2}{[E_1 - E]} \, 4 \left[1 + \left(\frac{E}{E_1}\right)^2 - \frac{2}{3} \frac{E}{E_1}\right] \left[\ln \frac{2 E_1 E}{mc^2 h \nu} - \frac{1}{2} - C(\gamma)\right]. \quad (A-5)$$

$C(\gamma)$ is plotted in Fig. 24.

Wheeler and Lamb [27] have developed an expression for the bremsstrahlung cross section for all the electrons in the atom. In the limit of complete screening this is

$$\left(\frac{d\sigma}{dE}\right)_{electrons} = \frac{z \alpha r_o^2}{[E_1 - E]} \, 4 \left\{ \left[1 + \left(\frac{E}{E_1}\right)^2 - \frac{2}{3} \frac{E}{E_1}\right] \ln \left(1440 \, z^{-\frac{2}{3}}\right) + \frac{1}{9} \frac{E}{E_1} \right\}. \quad (A-6)$$
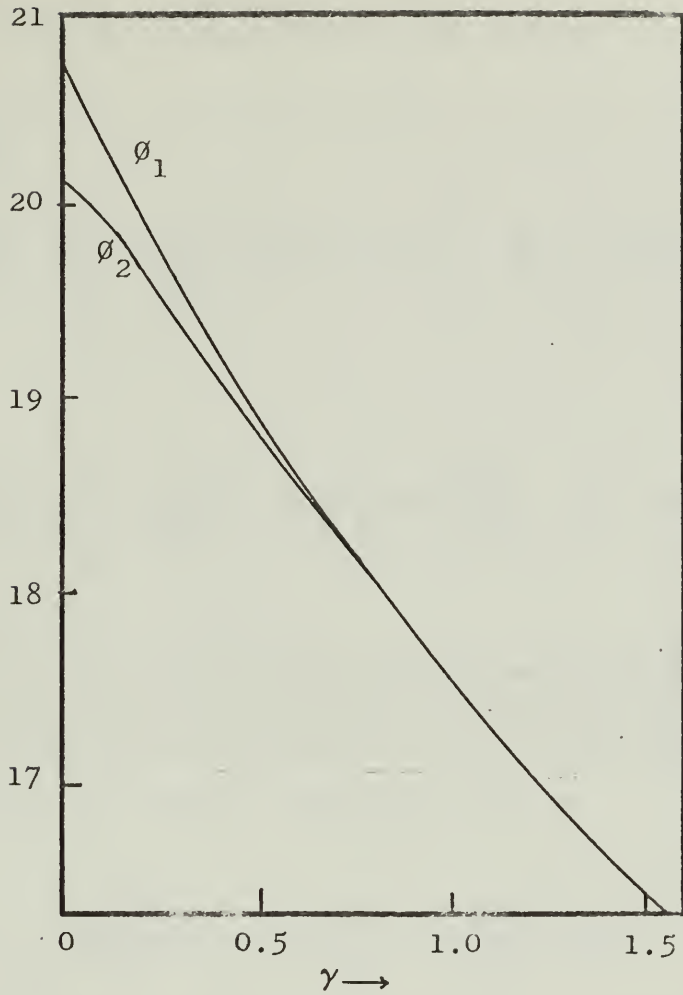
This leads to the Wheeler-Lamb factor ξ:

$$\xi = \frac{z \left(\frac{d\sigma}{dE}\right)_{electrons}}{\left(\frac{d\sigma}{dE}\right)_{nucleus}} \simeq \frac{\ln\left(1440 \, z^{-\frac{2}{3}}\right)}{\ln\left(183 \, z^{-\frac{1}{3}}\right)},$$

a term which occurs in many equations.

APPENDIX B.   SECONDARY EMISSION MONITORS

The secondary emission monitor (SEM) was first described by Tautfest and Fletcher [28]. An SEM consists of a set of thin metal foils placed in the beam so that the electrons are normally incident on the foils. Alternate foils are negatively biased to several hundred volts, so that secondary electrons ejected from the foils by the beam are collected on the positive plates. The resultant current, which is proportional to the beam current, can be monitored directly with an ammeter or collected on a capacitor used in conjunction with a vibrating reed electrometer to integrate the current. To determine the efficiency of an SEM, it must be compared to an absolute monitor such as a Faraday cup. Because of the high gamma and neutron radiation produced by the Faraday cup it cannot be used to monitor the beam during an experiment.

In most experiments performed at the NPGLINAC, a small, three-foil SEM was positioned inside the target chamber immediately downstream of the target, with a larger SEM outside the target chamber, but under continuous vacuum. The latter is used to integrate the beam current, while the small SEM monitored the beam current with a Beckman ammeter.

It was found that this arrangement is not satisfactory for experiments involving targets of different thickness. As the thickness of the target was increased, the current of each SEM was observed to increase (an increase of about 15% was noted for

a .25 inch carbon target for an incident energy of 35 MeV)[9]. To avoid this problem, the small SEM was moved upstream of the scattering target and used to integrate the current, while the large SEM was used with a Beckman ammeter.

The upstream SEM, composed of three aluminum foils .0025 inches thick, is actually a scatterer and served to increase the beam spot size. But even with the upstream SEM, and at low energies (35 MeV), the spot size never exceeded 3/16 inch in diameter. The primary disadvantage of this arrangement was that the target chamber, and thus the SEM, was occasionally exposed to air. However, the vacuum was attained at least eight hours before beginning the experiment and maintained below 2×10^{-5} mm Hg.

It has been reported by several authors [29,30] that the efficiency of these monitors changes significantly when first exposed to the beam. A graph of the SEM efficiency as a function of time is shown in Fig. 25. On these runs the beam current was held constant at 8×10^{-8} amp. The efficiency settled down to a constant value ($\pm$ 1.5%) after, at most, two hours exposure to the beam.

More important is the SEM efficiency as a function of beam current, since the beam current had to be changed considerably from thin to thick targets during each run. Bumiller and Dally [30]

---

[9] This increase is thought to be due to additional secondary electrons produced in the target which are collected by the SEM.

Fig. 25.
SEM efficiency vs.
exposure to beam

Fig. 26.
SEM efficiency vs.
beam current

59
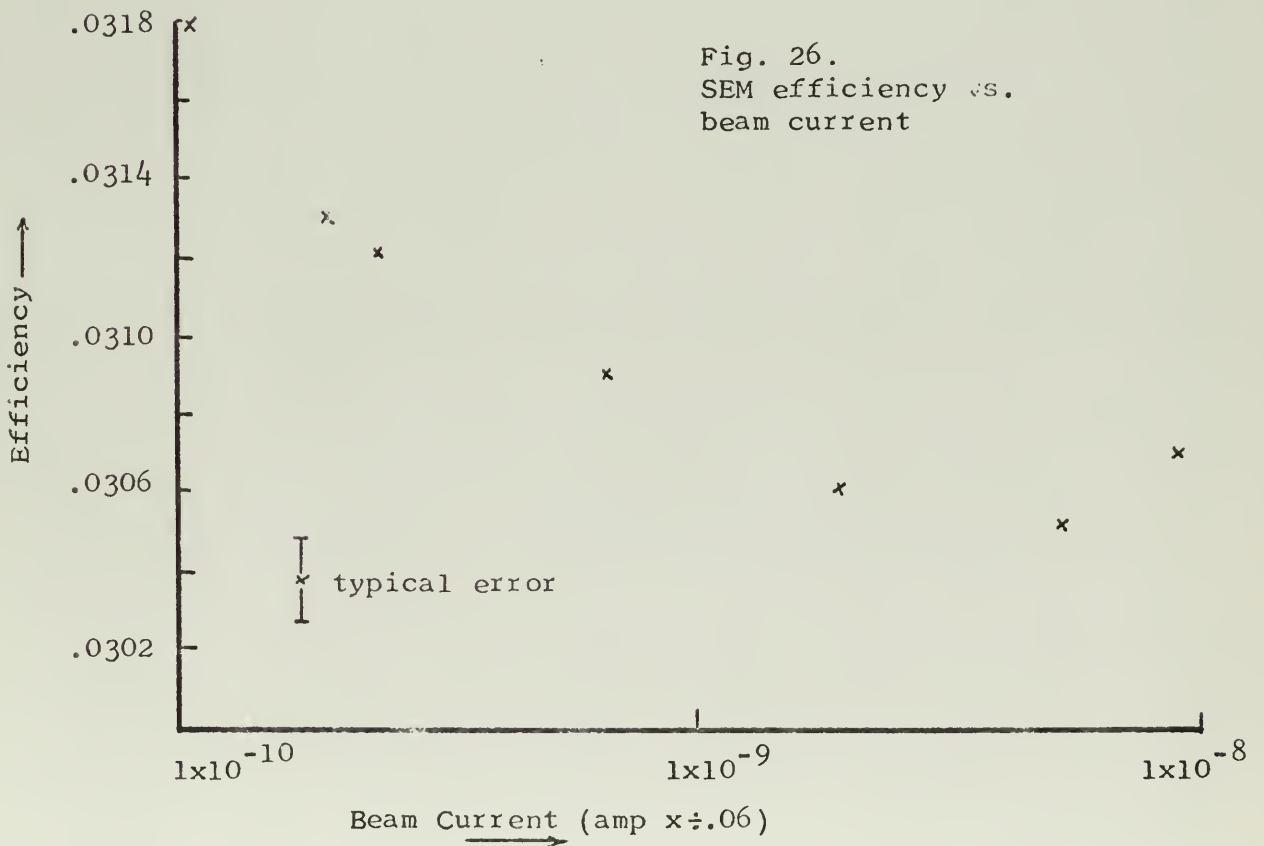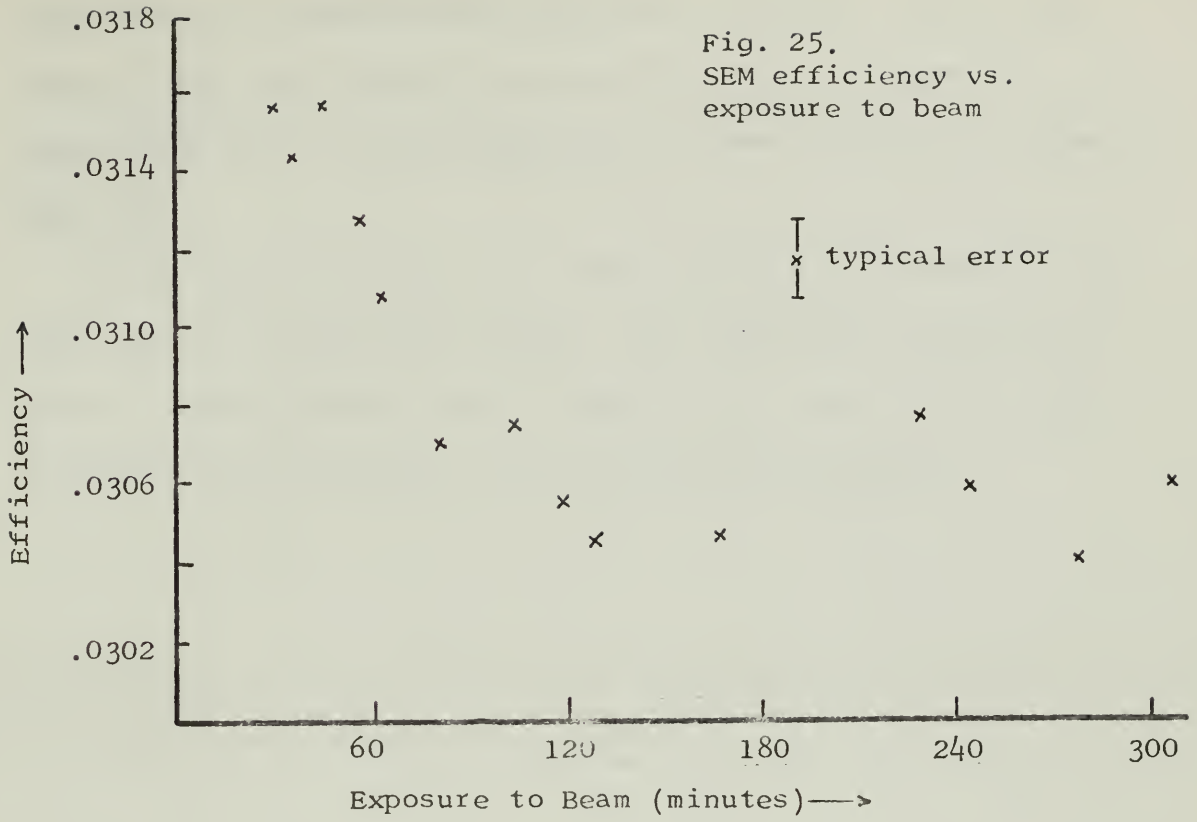
have reported a decreasing efficiency of 10% for one of their SEMs as the beam current decreased two orders of magnitude. We apparently see a reverse dependence on beam current, as shown in Fig. 26.

It is still not clear if a correction should be applied to the data to include this effect. This was wholly unexpected, and if correct, would tend to increase the slope of the cross section versus thickness curves described previously.

APPENDIX C.   SCATTERING WITHIN THE SPECTROMETER

The most persistent problem encountered during this experiment was a "ghost" of the elastic peak seen on the radiation tail of the peaks. The manifestation of this effect is the detection of extraneous electrons, primarily in channels eight, nine and ten, when the spectrometer is driven at least two percent below the energy of the elastic peak. A typical example of this effect is the thick target spectrum illustrated in Fig. 27. This problem can be minimized by the use of thin targets, where, in most cases, the peak can be measured to four half-widths without a major shift of the spectrometer.

It was first thought that this effect was due to scattering through the upper portion of an aluminum flange holding a vacuum window to the "snout" of the spectrometer. Initially a 1-1/8 inch block of lead was placed at the top of the snout to attempt to absorb the undesired electrons. This served only to increase the overall background. Then the flange was milled to one-half its original thickness with sharp edges filed so as not to interfere with the beam. This also showed no noticeable effect. The snout is illustrated in Fig. 28.

The rotating coil of the fluxmeter extends about two inches into the vacuum chamber of the spectrometer. It was removed for a single run to examine its contribution to the "ghosts". No change was noted.

Fig. 27.
Typical thick target spectrum showing
"ghost" of the elastic peak
.13" Aluminum, E_1 = 35.0 MeV

62

Fig. 28.
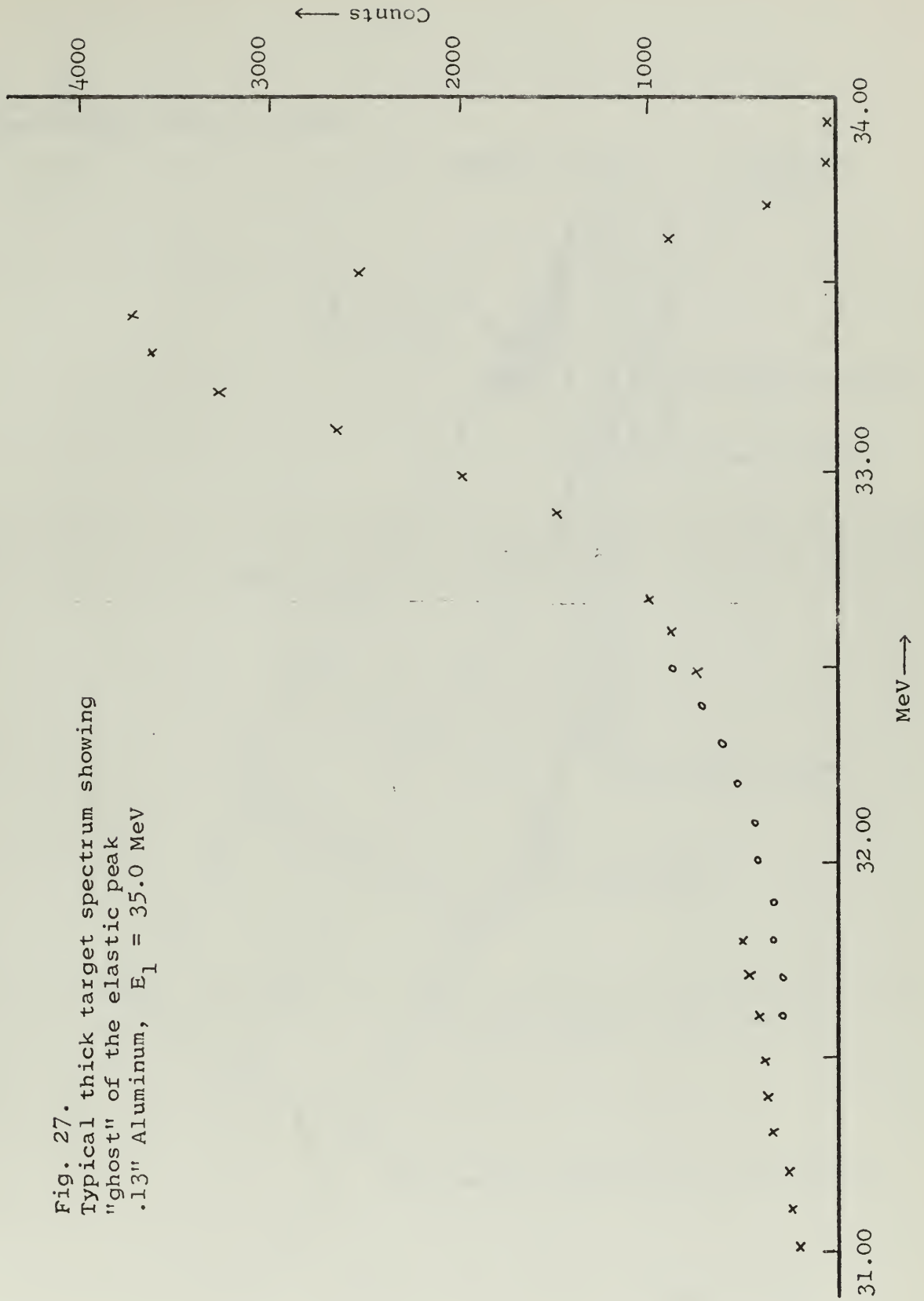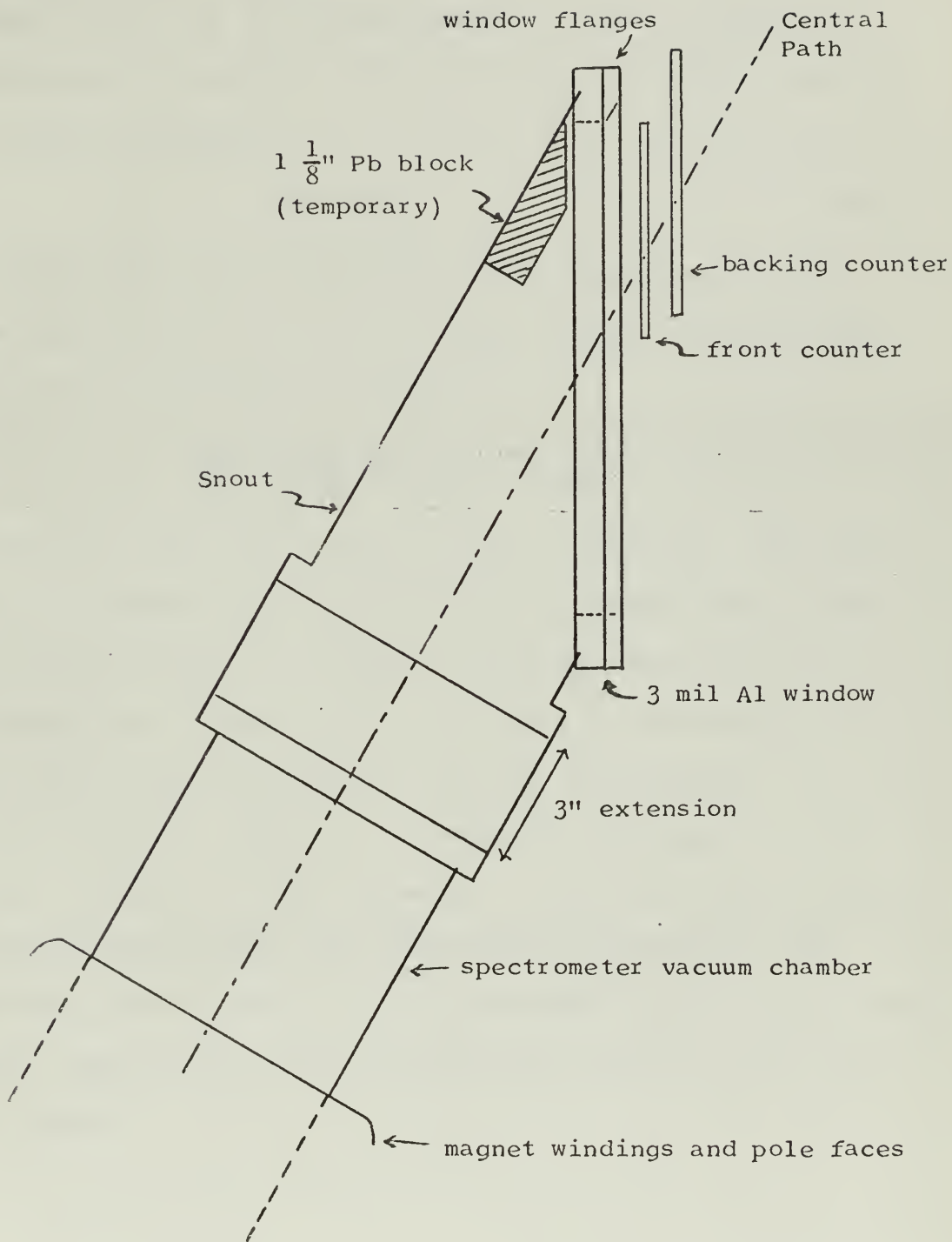Spectrometer Snout Assembly

window flanges

Central Path

$1 \frac{1}{8}$" Pb block
(temporary)

←backing counter

←front counter

Snout

←3 mil Al window

3" extension

←spectrometer vacuum chamber

←magnet windings and pole faces

Scale 1:.25

63

It is now believed that these extraneous electrons are due
to a small angle scattering of electrons which comprise the
elastic peak, as they graze the walls of the snout and a small
overhang at the top of the spectrometer. Order of magnitude
calculations can be made of the position of the elastic peak by
the dispersion formula

$$\frac{\Delta p}{p} = \frac{a/r}{D} \, . \tag{5-1}$$

For 35 MeV electrons to be shifted three inches up the focal
plane (where they first hit the flange) a shift in the central
energy of the spectrometer amounting to

$$\frac{\Delta p}{p} \simeq \frac{3/16}{3.92} \simeq 4.7\% = 1.5 \text{ MeV.}$$

is required. This corresponds to what is observed. Since this
effect is observed as the spectrometer is stepped down as much
as six percent more, it is unlikely that the ghosts are due to
scattering from a single point, but rather scattering over a
large region such as the entire top wall of the snout.

It would seem reasonable to construct a new snout of the
greatest possible vertical dimension. This would serve to move
scattering areas as far from the counters as possible. Any
scattering from the walls of the spectrometer cannot be corrected;
however, lowering the counters would help remove them from the
worst region.

LIST OF REFERENCES

1. R. Hofstadter, *Rev. Mod. Phys.*, 28, 214 (1956).

2. R. Hofstadter, *Ann. Rev. Nucl. Sci.*, 7, 231 (1957).

3. M.T. Barnett and W.J. Cunneen, Naval Postgraduate School Thesis, 1966.

4. P.N. Midgarden, Naval Postgraduate School Thesis, 1967.

5. L. Landau, *J. Phys. USSR*, 8, 201 (1944).

6. K.S. Symon, Harvard University Thesis, 1948.

7. D.B. Isabelle and G.R. Bishop, *Nucl. Phys.*, 45, 209 (1963).

8. B. Rossi, *High Energy Particles*, (Prentice-Hall, New York, 1952), p. 35.

9. H. Breuer, *Nucl. Inst. Meth.*, 33, 226 (1965).

10. O. Blunk, S. Leisegang, *Z. Physi*, 128, 500 (1950).

11. R.M. Sternheimer, *Phys. Rev.*, 103, 511 (1956).

12. J. Schwinger, *Phys. Rev.*, 76, 790 (1949).

13. Y.S. Tsai, *Phys. Rev.*, 122, 1898 (1961).

14. K. Mitchell, *Phil. Mag.*, 40, 351 (1949).

15. D.R. Yennie and H. Suura, *Phys. Rev.*, 105, 1378 (1957).

16. L.C. Maximon, *Rev. Mod. Phys.*, 41, 193 (1969).

17. Saskatchewan Accelerator Laboratory Report No. 4, *The Radiation Correction a Review of the Theory and Some Calculated Values*, by H. Breuer, December 1964.

18. L.W. Mo and Y.S. Tsai, *Rev. Mod. Phys.*, 41, 205 (1969).

19. H. Bethe and W. Heitler, *Proc. Roy. Soc. (London)*, A146, 83 (1934).

20. W. Heitler, *The Quantum Theory of Radiation* (Oxford University Press, London, 1954); 3rd ed., p. 224 and p. 378.

21. H.A. Bethe, Proc. Cambridge Phil. Soc., 30, 524 (1954).

22. H.A. Bethe and J. Ashkin, in Experimental Nuclear Physics, E. Segre, Ed. (John Wiley & Sons, Inc., New York, 1953), p. 265.

23. L.D. Oberdier, Naval Postgraduate School Thesis, 1967.

24. L.R. Suelzle, Stanford University Thesis, 1967.

25. H.L. Crannel and L.R. Suelzle, Nucl. Inst. Meth., 44, 133 (1966).

26. F.A. Bumiller (private communication, 1970).

27. J.A. Wheeler and W.E. Lamb, Phys. Rev., 55, 858 (1939).

28. G.W. Tautfest and H.R. Fletcher, Rev. Sci. Inst., 26, 229 (1955).

29. L.A.L. Report No. 1033, Factors Influencing the Stability of Secondary Electron Monitors, by D.B. Isabelle and Ph. Roy, 1962.

30. F.A. Bumiller and E.G. Dally, Proceedings of the International Conference on Instrumentation in High Energy Physics (Berkeley 1960), (Interstate Ed., New York, 1961, p. 305.

INITIAL DISTRIBUTION LIST

No. Copies

1. Defense Documentation Center   2
    Cameron Station
    Alexandria, Virginia 22314

2. Library, Code 0212   2
    Naval Postgraduate School
    Monterey, California 93940

3. Assoc. Professor Fred R. Buskirk   10
    Department of Physics (Code 61 Bs)
    Naval Postgraduate School
    Monterey, California 93940

4. LT John A. Gordon, USAF   1
    225 Hazel Street
    West Plains, Mo. 65775

5. AFIT-CI   1
    Wright-Patterson AFB, OH 45433

THIS PAGE INTENTIONALLY LEFT BLANK

DOCUMENT CONTROL DATA · R & D

(Security classification of title, body of abstract and indexing annotation must be entered when the overall report is classified)

1 ORIGINATING ACTIVITY *(Corporate author)*	2a. REPORT SECURITY CLASSIFICATION
Naval Postgraduate School	Unclassified
Monterey, California 93940	2b. GROUP

3 REPORT TITLE

Ionization and Radiative Corrections to Elastic Electron Scattering

4. DESCRIPTIVE NOTES *(Type of report and inclusive dates)*

Master's Thesis; June 1970

5. AUTHOR(S) *(First name, middle initial, last name)*

John A. Gordon

6. REPORT DATE	7a. TOTAL NO. OF PAGES	7b. NO. OF REFS
June 1970	67	30
8a. CONTRACT OR GRANT NO.	9a. ORIGINATOR'S REPORT NUMBER(S)	
b. PROJECT NO.		
c.	9b. OTHER REPORT NO(S) *(Any other numbers that may be assigned this report)*	
d.		

10. DISTRIBUTION STATEMENT

This document has been approved for public release and sale; its
distribution is unlimited.

11. SUPPLEMENTARY NOTES	12. SPONSORING MILITARY ACTIVITY
	Naval Postgraduate School
	Monterey, California 93940

13. ABSTRACT

The theory of the ionization and radiative corrections to electron scattering
cross sections has been reviewed to determine the formulas most valid for
the experimental arrangement at the NPGLINAC. Experimentally it has been
determined that the corrections most nearly account for undetected electrons
when the lower limit of the measured scattering spectrum is at least four
half-widths below the peak of the spectrum. It has also been found that
the corrections, most likely the Bethe-Heitler correction, induce a positive
error of several percent to the cross-section when thick targets are used.

DD ,FORM,,1473 (PAGE 1)
1 NOV 65

S/N 0101-807-6811

69

A-31408

14 KEY WORDS	LINK A		LINK B		LINK C	
	ROLE	WT	ROLE	WT	ROLE	WT
Bethe-Heitler correction						
Bremsstrahlung						
electron scattering						
ionization correction						
Landau straggling						
radiative corrections						
Schwinger correction						

DD FORM 1473 (BACK)
1 NOV 65

S/N 0101-807-6821

70

Unclassified

Security Classification

A-31409